BLOCK TRANSMISSIONS ON ORTHOGONAL CARRIERS

A THESIS SUBMITTED TO
THE GRADUATE SCHOOL OF NATURAL AND APPLIED SCIENCES
OF
MIDDLE EAST TECHNICAL UNIVERSITY

BY

AYHAN YAZICI

IN PARTIAL FULFILLMENT OF THE REQUIREMENTS
FOR
THE DEGREE OF MASTER OF SCIENCE
IN
ELECTRICAL AND ELECTRONICS ENGINEERING

AUGUST 2005

Approval of the Graduate School of Natural and Applied Sciences

Prof. Dr. Canan ÖZGEN
Director

I certify that this thesis satisfies all the requirements as a thesis for the degree of Master of Science.

Prof.Dr. İsmet ERKMEN
Head of Department

This is to certify that we have read this thesis and that in our opinion it is fully adequate, in scope and quality, as a thesis for the degree of Master of Science.

Prof. Dr. Buyurman BAYKAL
Supervisor

Examining Committee Members

Assoc. Prof. Dr. Melek YÜCEL	(METU, EE)	_____
Prof. Dr. Buyurman BAYKAL	(METU, EE)	_____
Assoc. Prof. Dr. Temel Engin TUNCER	(METU, EE)	_____
Dr. Özgür B. AKAN	(METU, EE)	_____
Dr. Emre AKTAŞ	(Hacettepe University, EE)	_____

I hearby declare that all information in this document has been obtained and presented in accordance with academic rules and ethical conduct. I also declare that, as required, I have fully cited and referenced all material and results that are not original to this work.

Name, Last name : AYHAN YAZICI

Signature :

ABSTRACT

BLOCK TRANSMISSIONS ON ORTHOGONAL CARRIERS

Yazıcı, Ayhan
M.Sc., Department of Electrical And Electronics Engineering
Supervisor: Prof. Dr. Buyurman Baykal

August 2005, 78 pages

Orthogonal Frequency Division Multiplexing (OFDM) and Single Carrier Block Transmissions (SCBT) are located at the two opposite edges of block transmission concept. In this thesis a system which lies between OFDM and SCBT is proposed. The new system, namely Block Transmissions on Orthogonal Carriers (BTOC), can be considered as a hybrid form of OFDM and SCBT. BTOC system is investigated under the redundant filterbank precoders and equalizers framework. Peak to average power ratio (PAPR) of BTOC is formulated and compared with the PAPRs of OFDM and SCBT. Effect of frequency offset for BTOC is investigated and comparison between OFDM, SCBT, and BTOC is presented. Simulation results of Zero Padded OFDM (ZP-OFDM), SCBT, and BTOC are included.

Keywords: OFDM, precoding, redundant filterbank precoders, single carrier block transmissions, carrier frequency offset, peak-to-average power ratio.

ÖZ

DİKGEN TAŞIYICILAR ÜZERİNDEN BLOK İLETİMİ

Yazıcı, Ayhan
Yüksek Lisans, Elektrik - Elektronik Mühendisliği Bölümü
Tez Yöneticisi: Prof. Dr. Buyurman Baykal

Ağustos 2005, 78 sayfa

Dikgen Frekans Bölüşümlü Çoğullama (OFDM) ve Tek Taşıyıcı Blok İletimi (SCBT) blok iletimi kavramının iki karşıt ucunda yer almaktadır. Bu tezde, OFDM ve SCBT arasında yer alan bir sistem önerilmektedir. Yeni sistem, yani Dikgen Taşıyıcılar üzerinden Blok İletimi (BTOC), OFDM ve SCBT'nin hibrit bir formu olarak düşünülebilir. BTOC sistemi fazlalık filtre bankası ön kodlayıcıları ve eşitleyiciler çatısı altında incelenmiştir. BTOC'un tepe ortalama güç oranı (PAPR) formüle edilmiş ve OFDM ve SCBT'nin PAPR'ları ile karşılaştırılmıştır. BTOC için frekans kayması etkisi incelenmiş ve OFDM, SCBT ve BTOC arasında bir karşılaştırma sunulmuştur. Sfr Eklemeli OFDM (ZP-OFDM), SCBT ve BTOC simülasyon sonuçları dahil edilmiştir.

Anahtar sözcükler: OFDM, ön kodlama, fazlalık filtre bankası ön kodlayıcıları, tek taşıyıcı blok iletimi, taşıyıcı frekans kayması, tepe ortalama güç oranı.

ACKNOWLEDGMENTS

First of all, I would like to thank my supervisor Prof. Dr. Buyurman Baykal for his guidance, support, advices and innovative ideas throughout my thesis. It is a big chance for me to work with him. I hope I will go on further with his invaluable guidance.

Being in the lead Dr. S. Gökhun Tanyer my special thanks go to my colleagues from TÜBITAK-UEKAE/İLTAREN for their support, trust and understanding.

Also, I want to express my gratitude to my all friends.

My dear family thanks for past, thanks for now and thanks for future...

I would like to thank to my fiance, Aytül Çatal for her love, encouragement, inspiration and understanding.

TABLE OF CONTENTS

LIST OF TABLES

LIST OF FIGURES

CHAPTER 1

INTRODUCTION

1.1 Background

Redundancy at the transmitter is an effective way to combat interblock interference (IBI) and intersymbol interference (ISI) [1] for block transmissions. This makes block transmissions a highly potential technique for high data rate systems. In order to investigate block transmission techniques and equalizer structures a framework which covers existing modulation schemes is needed. In [1] derivation of such a framework, representation of existing modulation schemes (i.e. OFDM, DMT, TDMA, FDMA, CDMA) under the framework, channel identifiability conditions, and design of zero-forcing equalizer for the framework are given. In [2], blind channel estimation algorithm and minimum mean square error equalizer design are given for the framework. So, this framework becomes an important tool when designing and analyzing a block transmissions scheme.

One of the commonly known block transmissions scheme is OFDM. OFDM has been chosen as the modulation technique in digital audio broadcast (DAB) and digital video broadcast (DVB) standards of Europe [3]. OFDM has also been chosen in IEEE802.11a, and the HIPERLAN/2 standards for local area mobile wireless networks [3].

Although OFDM is a promising technique for high data rate transmissions on fading channels, it has some serious problems. These problems have taken attention from OFDM to single carrier transmissions. Single carrier block

transmissions can be considered as transmitting a burst of symbols and then using guard interval on a single carrier. Use of cyclic prefix and frequency domain equalizers in single carrier systems, made single carrier systems to be compared with OFDM. In [4], [5], [6] frequency domain equalization of single carrier system and its comparison with OFDM is discussed. In [8] and [9] use of cyclic prefix as guard interval for single carrier systems is considered. In [10] capacity comparison of OFDM and single carrier system with frequency domain equalization is done.

A detailed comparison between OFDM and single carrier block transmissions is made in [3]. Another comparison between OFDM and single carrier block transmissions is made in [11]. In [11], why Cambridge Broadband has chosen to use single carrier modulation instead of OFDM for the VectaStar 3500 broadband fixed wireless access system is discussed. Comparison between single carrier and OFDM in [3] and [11] is based on nearly same subjects.

Considering OFDM and SCBT in time-frequency domain, they can be considered as they are located at two opposite edges. One of the two edges corresponds to OFDM and it means transmitting symbols on more than one carrier at the same time interval and using guard interval at the end of each symbol on each carrier. The other edge corresponds to SCBT and it means transmitting symbols on one carrier and after transmitting a number of symbols guard interval is used. So, there is a gap between OFDM and SCBT. This gap can be filled with a modulation technique which transmits symbols on more than one carrier and on each carrier it transmits a number of symbols then it uses guard interval on each carrier. This modulation technique is called as Block Transmissions on Orthogonal Carriers (BTOC). Investigation of BTOC will be made under the block transmissions framework proposed in [1] in this thesis.

1.2 Thesis Outline

In this thesis BTOC is derived and investigated as an alternative modulation technique to OFDM and single carrier block transmissions. The three modulation techniques -OFDM, single carrier block transmissions, and BTOC- are evaluated and compared using the common framework.

In Chapter 2 the redundant filterbank transceiver system model is reviewed. Block transmission concept is discussed first. After explaining the general structure of the model mathematically, equalizer design for the model is presented. The considered equalizer structures are zero forcing equalizer (ZF) and minimum mean square error equalizer. Two channel estimation algorithms are presented after the explanation of equalizer design. Blind channel estimation algorithm derived for the redundant filterbank transceiver model in [2] is presented first. The algorithm is described for both noiseless case and noisy case. The other channel estimation algorithm is training based channel estimation algorithm. In order to describe the algorithm, first a mathematical channel model, which is called basis extension model (BEM), is presented. The channel estimation algorithm is discussed based on the presented channel model.

Chapter 3 reviews the basics of OFDM. After a qualitative explanation of OFDM, mathematical description of OFDM and OFDM signal generation is presented. Representation of ZP-OFDM under the redundant filterbank transceiver framework is given following the general OFDM system model. After discussing OFDM the concept of SCBT and different guard interval types for SCBT are explained. The redundant filterbank transceiver model of SCBT is also given.

The proposed system, block transmissions on orthogonal carriers (BTOC), is investigated in Chapter 4. In the chapter the concept of BTOC is given. After the derivation of redundant filterbank representation of BTOC,

peak-to-average power ratio (PAPR) of BTOC is derived and it is compared with the PAPRs of OFDM and SCBT. Effect of frequency offset on performance of OFDM, SCBT, and BTOC is also investigated.

In Chapter 5 simulation results of ZP-OFDM, SCBT, and BTOC for different channels, different equalizers, different channel estimation methods, and different parameters are given and compared.

CHAPTER 2

System Model

2.1 Introduction

Block transmission schemes are used in many modern communication systems. The basic idea of block transmissions is dividing the input data stream into equal length blocks and transmitting each block with some redundancy. This idea is shown in Figure 2.1 schematically.

In the figure, length of the data sequence is 32 symbols. Symbols in the data sequence are grouped into length 8 blocks and redundancy is added to the blocks. Then the blocks are transmitted sequentially.

Some existing block transmission schemes are orthogonal frequency division multiplexing, coded-OFDM, discrete multitone, and pseudo random or wavelet based precoded transmissions for code division or discrete-wavelet multiple access [1].

In [1] and [2] a multirate filterbank transceiver model is proposed. The proposed model is a useful framework to model various block transmissions schemes. In order to evaluate performance of BTOC and compare its performance with existing modulation schemes, multirate transceiver model is used in this thesis. Using the multirate transceiver model allows comparison of BTOC and other modulation schemes under the same platform.

In this chapter multirate filterbank transceiver model is described. After describing the model, zero-forcing (ZF) and minimum mean square error (MMSE) equalizer designs for the system model will be given. Also, two

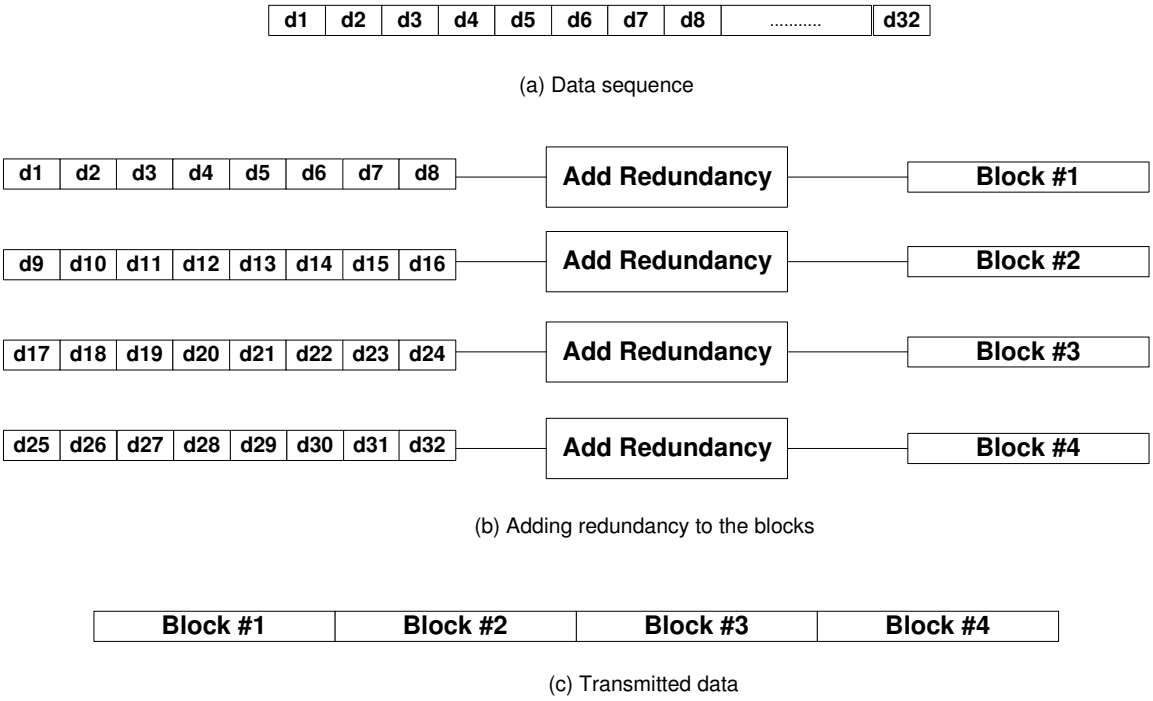

Figure 2.1: Block data generation

channel estimation algorithms for the system model, blind channel estimation algorithm and training based channel estiamtion algorithm, will be reviewed since these algorithms are used in the simulations.

2.2 Multirate Filterbank Transceiver Model

The multirate transceiver model derived in [1] is shown in Figure 2.2 schematically. All the representations here about the model is the same as in [1] except some additions. At the transmitter side of the model the incoming data sequence is divided into M substreams. This operation can be considered as a serial-to-parallel conversion or blocking in which each block contains M symbols. In the model the advance elements denoted by zs and

downsamplers act as serial-to-parallel converter. Downsamplers downsamples the input sequence by M. After downsamplers upsamplers are placed. These upsamplers upsamples the downsamplers' outputs by P. This means that in every branch upsampler inserts $P-1$ zeros after the data symbol. The input sequence, downsamplers' outputs and upsamplers' outputs are shown in Figure 2.3.

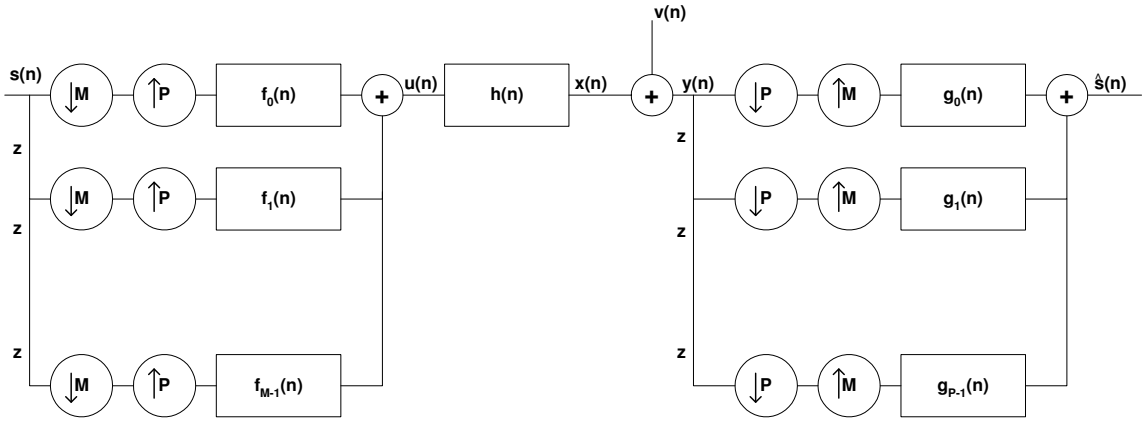

Figure 2.2: Multirate filterbank transceiver model

In Figure 2.2 the input data stream is represented by $s(n)$. The output of mth downsampler is $s_m(n) := s(nM + m)$. In this representation $s_m(n)$ represents the mth symbol in the nth block. The output of the mth upsampler is

$$d(n) = \sum_{i=-\infty}^{\infty} s(iM + m)\delta(n - iP) \tag{2.1}$$

In Figure 2.2, $f_m(n)$ represents the mth transmit filter's impulse response. The filters are driven by the output of the upsamplers. So, the output of mth filter is the convolution sum of the output of the mth upsampler and the impulse response of the mth filter. Let $c_m(n)$ denote the mth filter's output at sample n. $c_m(n)$ can be written as

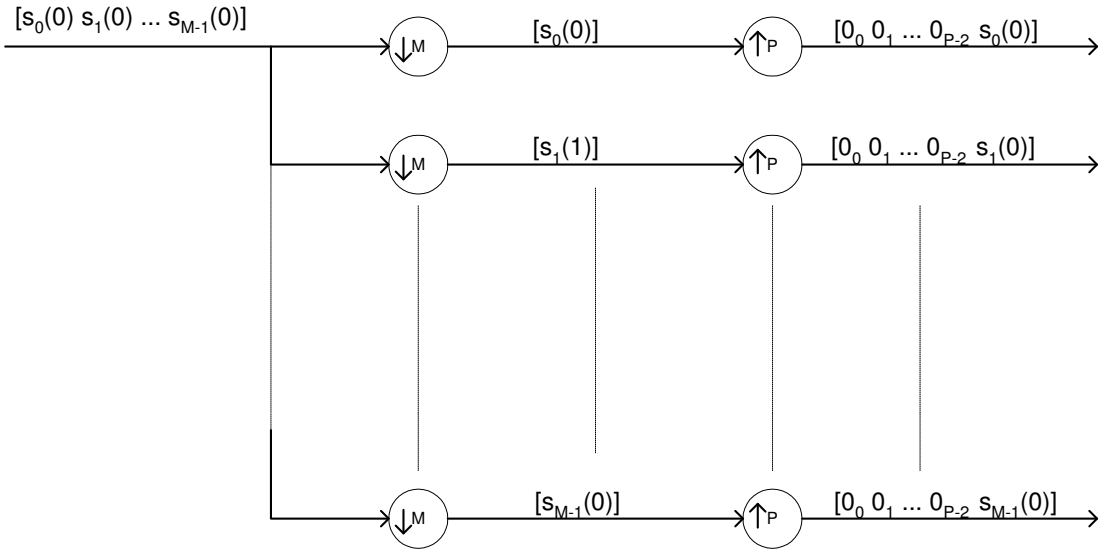

Figure 2.3: Signals at the downsamplers output and upsamplers output

$$c_m(n) = f_m(n) * d(n) = \sum_{i=-\infty}^{\infty} s(iM+m) f_m(n-iP). \tag{2.2}$$

Transmitter output is the sum of the M filters' outputs. Using (2.2) the transmitter output can be written as

$$u(n) = \sum_{m=0}^{M-1} \sum_{i=-\infty}^{\infty} s(iM+m) f_m(n-iP). \tag{2.3}$$

The transmitted signal $u(n)$ is passed through a linear time-invariant channel whose impulse response is $h(n)$. Additive Gaussian noise is added to the system at the output of the channel. So the received signal at the receiver is

$$
\begin{aligned}
y(n) &= x(n) + v(n) = \sum_{l=-\infty}^{\infty} h(l)u(n-l) + v(n) \\
&= \sum_{m=0}^{M-1} \sum_{i=-\infty}^{\infty} s(iM+m) \cdot \sum_{-\infty}^{\infty} h(l) f_m(n-l-iP) + v(n) \qquad (2.4)
\end{aligned}
$$

At the receiver, length P input blocks are converted to length M blocks with advance elements, downsamplers, and upsamplers. After this conversion the signals are fed to the P receive filters. The impulse response of the pth receive filter is represented by $g_p(n)$. The outputs of the receive filters are summed to produce the estimate of the transmitted symbols, $\hat{s}(n)$.

The receiver output, $\hat{s}(n)$, can be written as

$$
\hat{s}(n) = \sum_{p=0}^{P-1} \sum_{=-\infty}^{\infty} y(jP+p) g_p(n-jM). \qquad (2.5)
$$

Input/output relationship of the system will be used in vector form in order to ease the representation. Each input block is considered as a vector whose dimension is $M \times 1$. Vector form of one block can be written as

$$
\mathbf{s}(n) := (s(nM), s(nM+1), \cdots, s(nM+M-1))^T. \qquad (2.6)
$$

Like $s(n)$, $\hat{s}(n)$ can also be represented as a $M \times 1$ vector. Vector form of the estimated data block is

$$
\hat{\mathbf{s}}(n) := (\hat{s}(nM)\hat{s}(nM+1), \cdots, \hat{s}(nM+M-1))^T \qquad (2.7)
$$

The output of the transmitter, $u(n)$, and the input of the receiver, $y(n)$, and the output of the channel, $x(n)$, can be written as $P \times 1$ vectors. So the vector forms of $u(n)$, $y(n)$, and $x(n)$ can be written as

$$
\hat{\mathbf{u}}(n) := (u(nP), u(nP+1), \cdots, u(nP+P-1))^T \qquad (2.8)
$$

$$\hat{\mathbf{y}}(n) := (y(nP), y(nP+1), \cdots, y(nP+P-1))^T \tag{2.9}$$

$$\hat{\mathbf{x}}(n) := (x(nP), x(nP-1), \cdots, x(nP+P-1))^T \tag{2.10}$$

respectively.

The vector form representations of (2.2) and (2.5) are given in (2.11) and (2.12) respectively [1].

$$\mathbf{u}(n) = \sum_{i=-\infty}^{\infty} \mathbf{F}_i \mathbf{s}(n-i) \tag{2.11}$$

$$\hat{\mathbf{s}}(n) = \sum_{j=-\infty}^{\infty} \mathbf{G}_j \mathbf{y}(n-j) \tag{2.12}$$

where

$$\begin{aligned} &\{\mathbf{F}_i\}_{p,m} := f_m(iP+p) \\ &m = 0, \cdots, M-1; p = 0, \cdots, P-1 \end{aligned} \tag{2.13}$$

$$\begin{aligned} &\{\mathbf{G}_j\}_{m,p} := g_m(jM+m) \\ &m = 0, \cdots, M-1; p = 0, \cdots, P-1 \end{aligned} \tag{2.14}$$

The input of the receiver, $\mathbf{y}$(n), can be written as

$$\mathbf{y}(n) = \mathbf{x}(n) + \mathbf{v}(n) = \sum_{l=-\infty}^{\infty} \mathbf{H}_l \mathbf{u}(n-l) + \mathbf{v}(n) \tag{2.15}$$

where $\mathbf{H}_l$s are

$$\mathbf{H}_l := \begin{pmatrix} h(lP) & \cdots & h(lP-P+1) \\ \vdots & \ddots & \vdots \\ h(lP+P-1) & \dots & h(lP) \end{pmatrix} \tag{2.16}$$

Considering (2.11), (2.15), and (2.16) the receiver output (2.12) can be rewritten as

$$\hat{\mathbf{s}}(n) = \sum_{j,l,i=-\infty}^{\infty} \mathbf{G}_j \mathbf{H}_l \mathbf{F}_i \mathbf{s}(n-l-i-j) + \sum_{j=-\infty}^{\infty} \mathbf{G}_j \mathbf{v}(n-j). \tag{2.17}$$

where (2.17), $\{F_i\}_{p,m} = f_m(iP+p)$ and $\{G_j\}_{m,p} = g_p(jM+m)$.

In [1] three assumptions are made for perfect symbol recovery with FIR filterbanks of order $Q-1$ in the absence of noise. These assumptions are:

a1) The channel is modeled as an Lth order FIR filter with $h(0)$, $h(L) \neq 0$.

a2) $P > M$ and $P > L$

a3) All of the M transmit filters are causal so that their impulse responses satisfy $\{f_m(n) = 0\}_{m=0}^{M-1}$ for $n < 0$. And length of the impulse response of each transmit filter is not longer than P which means, considering causality, $\{f_m(n) = 0\}_{m=0}^{M-1}$ for $n < 0$ and $n \geq P$. Also the receive filters are causal and of length QM.

As stated in [1], the assumptions a2) and a3) allow modeling the transmit filterbank as $\mathbf{F}_i = \mathbf{F}_0 \delta(i)$.

In [2] another assumption has also been made. This assumption is:

a4) Transmit filters have L trailing zeros. So, $\{f_m(n) = 0\}_{m=0}^{M-1} = 0$ for $M \leq n \leq P$. And the precoder filters are linearly independent.

According to the assumptions a3), a4) the transmit filterbank, precoder, can be written as

$$\mathbf{F}_0^T = (\mathbf{F}^T \mathbf{0}^T). \tag{2.18}$$

Also linear independence stated in assumption a4) implies $rank(\mathbf{F}) = M$. As stated in [2], this means guarantee of one-to-one symbol mapping and perfect recovery of symbols in the absence of noise.

Since the precoder inserts L zeros to the transmitted block, two consecutive blocks will not overlap, so interblock interference will not occur. In (2.17), the index of $\mathbf{H}_l$, l, represents interblock interference when $l \neq 0$. As an example $\mathbf{H}_1$ represents interblock interference between two consecutive blocks. According to the assumption a4), inserting L zeros at the end of each block, there will be only $\mathbf{H}_0$ in the equation (2.17). So the sum over l vanishes in (2.17). Also since $\mathbf{F}_i = \mathbf{F}_0 \delta(i)$ the sum over i also vanishes in (2.17). So, (2.17) can be rewritten as

$$\hat{\mathbf{s}}(n) = \sum_{j=-\infty}^{\infty} \mathbf{G}_j \mathbf{H}_0 \mathbf{F}_0 \mathbf{s}(n-j) + \sum_{j=-\infty}^{\infty} \mathbf{G}_j \mathbf{v}(n-j) \tag{2.19}$$

where the $P \times P$ channel matrix $\mathbf{H}_0$ is

$$\mathbf{H}_0 := \begin{pmatrix} h(0) & 0 & 0 & \cdots & 0 \\ \vdots & 0 & 0 & \cdots & 0 \\ h(L) & \cdots & \ddots & \cdots & \vdots \\ \vdots & \ddots & \cdots & \ddots & 0 \\ 0 & \cdots & h(L) & \vdots & h(0) \end{pmatrix} \tag{2.20}$$

The channel matrix in (2.20) is a Toeplitz matrix. The first column of the matrix is $(h(0) \cdots h(L)\ 0 \cdots 0)^T$ and the first row of the matrix is $(h(0)\ 0 \cdots 0)^T$.

Considering the assumptions, the output of the transmitter can be written as [1]

$$\mathbf{u}(n) = \mathbf{F}_0\mathbf{s}(n). \tag{2.21}$$

So the output of the channel, $\mathbf{x}(n)$ is

$$\mathbf{x}(n) = \mathbf{H}_0\mathbf{F}_0\mathbf{s}(n). \tag{2.22}$$

The signal at the receiver input is

$$\mathbf{y}(n) = \mathbf{H}_0\mathbf{F}_0\mathbf{s}(n) + \mathbf{v}(n). \tag{2.23}$$

where $\mathbf{v}(n)$ is additive white Gaussian noise.

As stated above, under the assumptions made, two consecutive blocks do not overlap. Also there is a one-to-one mapping between the transmitter input and the transmitter output. So, the received signal, $\mathbf{y}(n)$ is a sufficient statistic for $\mathbf{s}(n)$ [2]. Also the zero order receive filters are sufficient to decode the received signal. With this information in mind, $Q = 1$ holds. So each of P receive filters are all of length M. The receive filterbank matrix becomes $\mathbf{G}_j = \mathbf{G}_0\delta(j)$. The equation (2.19) takes the form

$$\hat{\mathbf{s}}(n) = \mathbf{G}_0\mathbf{H}_0\mathbf{F}_0\mathbf{s}(n-j) + \mathbf{G}_0\mathbf{v}(n-j). \tag{2.24}$$

As stated in [2], let

$$\mathbf{H} := \begin{pmatrix} h(0) & 0 & \cdots & 0 \\ \vdots & \ddots & \ddots & \vdots \\ h(L) & \ddots & \ddots & 0 \\ 0 & \ddots & \ddots & h(0) \\ \vdots & \ddots & \ddots & \vdots \\ 0 & \cdots & 0 & h(L) \end{pmatrix} \tag{2.25}$$

be the $P \times M$ Toeplitz channel matrix formed using the first M columns of $\mathbf{H}_0$. Considering (2.22) the following equation holds.

$$\mathbf{H}_0\mathbf{F}_0 = \mathbf{HF} \tag{2.26}$$

The received signal at the receiver input can be rewritten as

$$\mathbf{y}(n) = \mathbf{HFs}(n) + \mathbf{v}(n). \tag{2.27}$$

The estimated data block at the receiver output is

$$\hat{\mathbf{s}}(n) = \mathbf{GHFs}(n) + \mathbf{Gv}(n). \tag{2.28}$$

2.3 Equalizer Design

The design of the receive filterbank with receive filters $\{g_p(n)\}_{p=0}^{P-1}$ depends on the choice equalization strategy. Various equalization methods exist. Some of them are Viterbi's algorithm, linear equalization, iterative equalization, and decision-feedback equalization. Among these equalizers, linear equalizers are easy to implement and less complex than other equalizer structures. In this thesis two types of linear equalizers will be used. These equalizers are zero forcing(ZF) equalizer and minimum mean square error(MMSE) equalizer.

2.3.1 Zero Forcing Equalizers

Since the aim of equalization is to extract the data block $\mathbf{s}(n)$ from the received data vector $\mathbf{y}(n)$, taking inverse of $\mathbf{GHF}$ in (2.27) and multiplying the inverse with the received signal is an explicit way to equalize the channel effects on the transmitted signal and to recover the data block $\mathbf{s}(n)$. This

method is called zero forcing equalization. The name comes from the fact that in the absence of noise and with perfect channel knowledge, zero forcing equalizer recovers the data perfectly.

The formulation of zero forcing equalizer can be written as [2]

$$\mathbf{G}_{zf} = \mathbf{F}^{-1}\mathbf{H}^{\dagger} = \mathbf{F}^{-1}(\mathbf{H}^{H}\mathbf{H})^{-1}\mathbf{H}^{H} \tag{2.29}$$

where † represents pseudo inverse.

2.3.2 Minimum Mean Square Error Equalizers

As stated in 2.3.1 in the absence of noise zero forcing equalizers performs perfect symbol recovery. But in a noisy environment the performance of zero forcing equalizers degrades quickly with increasing noise. This characteristic of zero forcing equalizer makes it a good choice for high signal-to-noise ratio (SNR) environments. For low SNR conditions an equalizer much successful than zero forcing equalizer is needed. Minimum mean square equalizers preform better than zero forcing equalizers in low SNR environments. MMSE equalizers performs better than ZF equalizers in noisy environments.

In [2] and [12] formulation of MMSE equalizer for the system model described in Section 2.2 is given. The aim in MMSE equalizer is to minimize the mean square error between the input of the transmitter, $\mathbf{s}(n)$ and the output of the receiver, $\hat{\mathbf{s}}(n)$. The cost function that will be minimized is [2]

$$J(\mathbf{G}) := E\{tr[\mathbf{G}\mathbf{y}(n) - \mathbf{s}(n)][\mathbf{G}\mathbf{y}(n) - \mathbf{s}(n)]^{H}\}. \tag{2.30}$$

Since the task of the MMSE equalizer is to minimize the mean square error given in (2.30), the equalizer filterbank matrix $\mathbf{G}$ is the matrix which makes the gradient of (2.30) with respect to $\mathbf{G}$ 0. The solution for $\mathbf{G}$ is [2], [12]

$$\mathbf{G}_{mmse} = \mathbf{R}_{ss}\mathbf{F}^H\mathbf{H}^H(\mathbf{R}_{vv} + \mathbf{HFR}_{ss}\mathbf{F}^H\mathbf{H}^H)^{-1}. \tag{2.31}$$

In (2.31), $\mathbf{R}_{ss}$ is the correlation matrix of the input data $\mathbf{s}(n)$. $\mathbf{R}_{vv}$ is the covariance noise $\mathbf{v}(n)$.

In [2] it is shown that in the absence of noise, which means $SNR \rightarrow \infty$, the equalizer matrix which minimizes the mean square error is $\mathbf{G} = (\mathbf{HF})\dagger$. So in the absence of zero forcing equalizer minimizes the mean square error term in (2.30)

2.4 Channel Estimation

In 2.3 design of ZF equalizer and MMSE equalizer for block transmission were discussed. From (2.29) and (2.31) it is obvious that in the design of the equalizer channel knowledge is essential. Sometimes channel is known by the receiver. This situation is valid generally for constant channels. Especially for wireless channels the channel is not constant and it can not be known by the receiver all the time. But its main statistical characteristics may be known. So the channel has to be learned in a way to produce the equalizer filterbank matrix.

Various algorithms are produced for channel estimation. These algorithms can be classified into three main categories. These are:

1. Training based
2. Semi-blind
3. Blind

In training based channel estimation method, known symbols are transmitted among data symbols by the transmitter. The receiver first processes

the known symbols and then estimates the channel impulse response. The recovery of the data symbols are made later.

In 3.1 and 2.2, it is shown that some amount of redundancy is added to the transmitted block in order to combat intersymbol interference and to recover the transmitted data symbols. The redundancy introduced at the transmitter can be cyclic prefix or suffix, zero padding, known symbol padding. In zero padding case and in known symbol padding case the redundant symbols are same for all blocks. So, in terms of channel estimation, the redundancy introduced in zero padding and known symbol padding can be considered as fixed pilot blocks [13]. If the redundancy is in the form of known symbol padding than this channel estimation is called semi-blind channel estimation [13]. If the redundancy is in the form of zero padding the channel estimation algorithm using zero blocks is called blind channel estimation [2], [12].

In this thesis, training sequence based channel estimation and blind channel estimation will be investigated for the proposed system.

2.4.1 Blind Channel Estimation

In [2] and [12] a blind channel estimation algorithm is proposed for redundant filterbank precoders framework. In [14] a similar algorithm is discussed for space-time block precoded systems. This channel estimation algorithm will be used as the blind channel estimation algorithm in this work.

In [2] and [12], the blind channel estimation algorithm is proposed for both noiseless case and noisy case. In the following subsection the algorithm will be discussed for noiseless case. After discussing the noiseless case, blind channel estimation algorithm for noise case will be presented.

Blind Channel Estimation - Noiseless Case

In the description of the system model, it was shown that $\mathbf{x}(n) = \mathbf{HFs}(n)$. In [2] a collection of N $\mathbf{x}(n)$s are shown as

$$\mathbf{X}_N = (\mathbf{x}(0) \cdots \mathbf{x}(N-1)) = \mathbf{HFS}_N \tag{2.32}$$

where $M \times N$ matrix $\mathbf{S}_N$ is

$$\mathbf{S}_N := (\mathbf{s}(n) \cdots \mathbf{s}(N-1)). \tag{2.33}$$

Considering (2.25) if one channel coefficient is different than zero then $rank(\mathbf{H}) = M$ [2]. Considering this fact and the assumptions made, $rank(\mathbf{X}_N) = M$ holds [2]. Since $\mathbf{X}_N$ is a $P \times P$ matrix the nullity of $\mathbf{X}_N\mathbf{X}_N^H$ is $P - M = L$ [2]. $\mathbf{X}_N\mathbf{X}_N^H$ can be decomposed as [2]

$$\mathbf{X}_N\mathbf{X}_N^H = (\overline{\mathbf{U}}\widetilde{\mathbf{U}}) \begin{pmatrix} \sum_{M\times M} & \mathbf{0}_{M\times L} \\ \mathbf{0}_{L\times M} & \mathbf{0}_{L\times L} \end{pmatrix} \begin{pmatrix} \overline{\mathbf{U}}^H \\ \widetilde{\mathbf{U}}^H \end{pmatrix}. \tag{2.34}$$

In (2.34) columns of $\overline{\mathbf{U}}$ spans the nulls space of $\mathbf{X}_N$. The null space of $\mathbf{X}_N$ is orthogonal to the channel matrix $\mathbf{H}$ [2].

$$\widetilde{\mathbf{U}}^H\mathbf{H} = 0 \tag{2.35}$$

(2.35), is rewritten in [2] as

$$\mathbf{h}^H\boldsymbol{U} := \mathbf{h}^H(\boldsymbol{U}_1 \cdots \boldsymbol{U}_L) = \mathbf{0}^H \tag{2.36}$$

where $\boldsymbol{U}_l$ is an $(L+1) \times M$ Hankel matrix with the form as

$$\boldsymbol{U}_l = \begin{pmatrix} \tilde{u}_l(0) & \tilde{u}_l(1) & \cdots & \tilde{u}_l(P-L-1) \\ \tilde{u}_l(1) & \tilde{u}_l(2) & \cdots & \tilde{u}_l(P-L) \\ \vdots & \vdots & \vdots & \vdots \\ \tilde{u}_l(L) & \tilde{u}_l(L+1) & \cdots & \tilde{u}_l(P-1) \end{pmatrix} \tag{2.37}$$

The channel estimate comes from the solution of (2.36). So, from (2.36) channel estimate is the unique null eigenvector of $\boldsymbol{U}$. The unique null eigenvector of $\boldsymbol{U}$ (also channel estimate) equals the singular vector corresponding to the minimum singular value of $\boldsymbol{U}^H$ [15].

With this blind channel estimation algorithm the channel can be estimated up to a scalar ambiguity. This fact can be represented as

$$\hat{\mathbf{h}} = \alpha \mathbf{h}, \alpha \in \Re \tag{2.38}$$

Blind Channel Estimation - Noisy Case

The covariance matrix of noise, $\mathbf{R}_{vv}$, is assumed to be known in the noisy channel estimation case. If noise is not white, first it is whitened with using the factorization $\mathbf{R}_{vv} = \Phi_v \Phi_v^H$.

Covariance matrix of the received signal, $\mathbf{R}_{yy}$, is used in noisy case instead of $\mathbf{X}_N \mathbf{X}_N^H$ in the noiseless case. So the eigendecomposition of $\Phi_v^{-1} \mathbf{R}_{yy} \Phi_v^{-H}$ is used.

In order to obtain Φ_v from $\mathbf{R}_{vv}$, the Cholesky factorization can be used.

Let $\tilde{\mathbf{U}}_y^{\Phi}$ be a $P \times L$ matrix whose columns are L eigenvectors of $\Phi_v^{-1} \mathbf{R}_{yy} \Phi_v^{-H}$ corresponding to the smallest L eigenvalues. Considering the noiseless case, $\Phi^{-H} \tilde{\mathbf{U}}_y^{\Phi}$ can be used instead of $\tilde{\mathbf{U}}$. The remaining operations are the same in the noiseless case.

2.4.2 Training Based Channel Estimation

In Section 2.4.1, blind channel estimation was discussed. No redundant symbols were inserted for blind channel estimation. Another way to estimate the channel impulse response is training based channel estimation. In this method, known symbols are inserted to the data block to be transmitted. Inserted known symbols are called as training symbols or pilot symbols. Training symbols are passed through the channel whose impulse response is $h(n)$, and the resultant signal is received by the receiver. At the receiver the received signal is processed in order to extract the channel impulse response with the knowledge of the transmitted training symbols.

In [16], [17], [18], and [19] training based channel estimation methods are investigated for block transmission systems. In [16] and [17], training based channel estimation is discussed for frequency selective channels. However the channel estimation algorithm presented in [18] and [19] are for doubly-selective channels. This channel estimation algorithm will be used for training based channel estimation. Before describing this channel estimation algorithm, the channel model used in [18] and [19] has to be explained. After clarification of the channel model, the channel estimation algorithm is described.

Channel Model: Basis Extension Model

In [19] a channel model, namely basis extension model (BEM), to model time and frequency selective channels mathematically is proposed. This channel model is used to derive the channel estimation algorithm in [18] and [19].

The starting point of BEM channel model is the continuous time and continuous frequency impulse response of the channel. Using this impulse response, the discrete-time equivalent channel impulse response is formulated.

In [19], impulse response of the channel is given as

$$c^{(ch)}(t;\tau) = \sum_{\nu} \alpha_\nu(t) e^{j\theta_\nu(t)} \delta(\tau - \tau_\nu(t)). \tag{2.39}$$

In this equation ν is the index of sum of signals arriving with equal delay $\tau_\nu(t)$. $\alpha_\nu(t)$ and $\theta_\nu(t)$ are the amplitude and phase of the sum signal, respectively. The sum of signals arriving with equal delay $\tau_\nu(t)$ can be written in terms of individual signals as [19]

$$\alpha_\nu(t) e^{j\theta_\nu(t)} = \sum_{\nu} a_{\mu,\nu}(t) e^{j\phi_{\mu,\nu}(t)} e^{j2\pi f_{\mu,\nu}(t)t}. \tag{2.40}$$

In (2.40), μ is the index of signals with delay $\tau_\nu(t)$. $f_{\mu,\nu}(t)$, $\phi_{\mu,\nu}(t)$, and $a_{\mu,\nu}(t)$ are frequency offset, phase, and amplitude of the μth signal, respectively.

The effects of transmit and receive filters can be included into the channel impulse response. Defining $\psi(t)$ as the convolution of the transmit and receive filter, the resultant channel impulse response can be written as

$$c(t;\tau) = \sum_{\nu} \psi(\tau - \tau_\nu(t)) \sum_{\mu} a_{\mu,\nu}(t) e^{j\phi_{\mu,\nu}(t)} e^{j2\pi f_{\mu,\nu}(t)t} \tag{2.41}$$

The frequency domain representation of (2.41) is [19]

$$C(f;\tau) = \sum_{\nu} \psi(\tau - \tau_\nu) \sum_{\mu} a_{\mu,\nu}(n) e^{j\phi_{\mu,\nu}(n)} sinc(f - f_{\mu,\nu}(n)). \tag{2.42}$$

Since channel impulse response is needed for one block with N symbols, the frequency domain representation of the channel impulse response, (2.42) can be sampled in frequency domain with period $1/(NT_s)$. The frequency domain sampled form of (2.42) is

$$C(\frac{q}{NT_s};\tau) = \sum_{\nu} \psi(\tau - \tau_\nu(n)) \sum_{\mu} a_{\mu,\nu}(n) e^{j\phi_{\mu,\nu}(n)} sinc(\frac{q}{NT_s} - f_{\mu,\nu}(n))$$
$$q \in (-\infty, \infty) \quad (2.43)$$

Since maximum doppler shift limits the bandwidth of $C(\frac{q}{NT_s};\tau)$, it can be assumed that $C(\frac{q}{NT_s};\tau) = 0$ for $q \notin [-Q/2, Q/2]$, where $Q = 2\lceil f_{max} T_s N \rceil$. f_{max} represents the maximum doppler shift.

Impulse response of the channel can be written in time-domain using (2.43) as

$$c(t;\tau) = \sum_{q=-Q/2}^{Q/2} [\sum_{\nu} \psi(\tau - \tau_\nu(n)) \sum_{\mu} a_{\mu,\nu}(n) e^{j\phi_{\mu,\nu}(n)} sinc(\frac{q}{NT_s} - f_{\mu,\nu}(n))] e^{j2\pi \frac{q}{NT_S} t}. \quad (2.44)$$

Sampling (2.44) in t and τ gives the discrete-time channel impulse response for frequency selective - time selective channels. So the discrete time representation of frequency selective time selective fading channels is [19]

$$\begin{aligned} h(i;l) &= c(iT_s; lT_s) \\ &= \sum_{q=-Q/2}^{Q/2} [\sum_{\nu} \psi(lT_s - \tau_\nu(n)) \sum_{\mu} a_{\mu,\nu}(n) e^{j\phi_{\mu,\nu}(n)} \\ &\quad sinc(\frac{q}{NT_s} - f_{\mu,\nu}(n))] e^{j\frac{2\pi}{N} qi}. \end{aligned} \quad (2.45)$$

(2.45) can be written shortly as

$$h(i;l) = \sum_{q=-Q/2}^{Q/2} \bar{h_q}(n;l) e^{j\bar{\omega_q} i} \quad (2.46)$$

where

$$\bar{\omega}_q = 2\pi q/N \tag{2.47}$$

$$\bar{h}_q(n;l) = \sum_{\nu} \psi(lT_s - \tau_\nu(n)) \sum_{\mu} a_{\mu,\nu}(n) e^{j\phi_{\mu,\nu}(n)} \\ sinc(q/(NT_s) - f_{\mu,\nu}(n)), n = \lfloor i/N \rfloor . \tag{2.48}$$

From (2.46), in order to estimate the channel impulse response, values of $\bar{h}_q(n;l)$ has to be determined. So, in a channel estimation problem, when using BEM, there are $(Q+1)(L+1)$ unknown coefficients. In the subsequent subsection estimation of these $(Q+1)(L+1)$ parameters will be discussed.

Channel Estimation

In [18], optimal training for block transmissions was considered. The optimality of the training is in terms of optimal placement of pilots, optimal number of sub-blocks(will be explained later), and optimal power allocation.

Both in [19] and in [18] considered system is based on block transmissions. In [18], the training symbols inserted block is represented as

$$\mathbf{u}(k) = [\mathbf{s}_1^T(k), \mathbf{b}_1^T(k), \cdots, \mathbf{s}_P^T(k), \mathbf{b}_P^T(k)]^T. \tag{2.49}$$

In this representation $\mathbf{s}$'s represents information sub-blocks and $\mathbf{u}$'s represents training sub-blocks. Let $\mathbf{b} = [\mathbf{b}_1^T, \cdots, \mathbf{b}_P^T]$ and

$$\mathbf{y}_b = \mathbf{H}_b\mathbf{b} + \mathbf{w}_b. \tag{2.50}$$

$\mathbf{y}_b$ in (2.50) represents received signals due to transmitted training symbols. Channel estimation will be made using $\mathbf{y}_b$ and the knowledge of the transmitted training symbols, $\mathbf{b}$.

The product $\mathbf{H}_b\mathbf{b}$ in (2.50) can be written as [18], [19]

$$\mathbf{H}_b\mathbf{b} = \sum_{q=0}^{Q} \mathbf{D}_q\mathbf{B}\mathbf{h}_q = [\mathbf{D}_0\mathbf{B} \ \cdots \ \mathbf{D}_Q\mathbf{B}]\mathbf{h} \tag{2.51}$$

where $\mathbf{D}_q = diag[1, \ldots, exp(j\omega_q((Q+1)(L+1)-1))]$, $\mathbf{h}_q = [h_q(0) \cdots h_q(L)]$, and $\mathbf{B} = [\mathbf{B}_0 \cdots \mathbf{B}_Q]$. $\mathbf{B}_p$ is expressed as

$$\mathbf{B}_p = \begin{pmatrix} b_{p,L} & \cdots & b_{p,0} \\ \vdots & \cdots & \vdots \\ b_{p,(Q+1)(L+1)-1} & \cdots & b_{p,(Q+1)(L+1)-L-1} \end{pmatrix}$$

(2.50) can be expressed as [18]

$$\mathbf{y}_b = \Phi_b\mathbf{h} + \mathbf{w}_b \tag{2.52}$$

where

$$\Phi_b = \begin{pmatrix} \mathbf{D}_{0,1}^b\mathbf{B}_1 & \cdots & \mathbf{D}_{Q,1}^b\mathbf{B}_1 \\ \vdots & \cdots & \vdots \\ \mathbf{D}_{0,Q}^b\mathbf{B}_Q & \cdots & \mathbf{D}_{Q,Q}^b\mathbf{B}_P \end{pmatrix} \tag{2.53}$$

The channel can be estimated with the knowledge of Φ_b. There are two criterions to estimate the channel. One of these is zero-forcing and the other is minimum mean square error.

The zero forcing channel estimator is formulated as [19]

$$\hat{h} = (\Phi_b)^{-1}\mathbf{y}_b \tag{2.54}$$

and the minimum mean square error channel estimator is formulated as [19]

$$\hat{h} = \frac{1}{\sigma_\omega^2}(\mathbf{R}_h^{-1} + \frac{1}{\sigma_\omega^2}\Phi_b^H\Phi_b)^{-1}\Phi_b^H\mathbf{y}_b. \tag{2.55}$$

where σ_ω^2 is the noise variance and $\mathbf{R}_h$ is the channel autocorrelation matrix.

Optimal Training In the previous subsection training based channel estimation algorithm for block transmissions was discussed. In the algorithm, only obtaining the channel estimate from the received symbols and knowledge of the training symbols was considered. No consideration about the training symbols were take place. In this subsection properties of the training symbols will discussed.

In [18], the optimality of training symbols was discussed. The optimal design of training symbols were made in terms of

1. Optimal placement
2. Optimal number of sub-blocks
3. Optimal power allocation

Optimal Placement of Pilots The aim in the optimal placement of pilot tones is to minimize the mean square error between the channel impulse response and the estimated channel impulse response. The mean square error can be written as [18]

$$\sigma_{\hat{h}}^2 = \sum_m \frac{1}{[\mathbf{R}_h^{-1} + \frac{1}{\sigma_\omega^2}\Phi_b^H \Phi_b]_{m,m}} \geq \sum_m \frac{1}{[\mathbf{R}_h^{-1} + \frac{P_b}{\sigma_\omega^2}\mathbf{I}]_{m,m}} \tag{2.56}$$

Derivations of the optimal pilot placement is given in [18]. Only the resultant placement will be mentioned here. In order to obtain minimum MSE the structure of the transmitted block should be as follows [18]

$$\mathbf{u} = [\mathbf{s}_1^T \mathbf{0}_L^T b \mathbf{0}_L^T \cdots \mathbf{s}_P^T \mathbf{0}_L^T b \mathbf{0}_L^T]^T, b = \sqrt{\bar{P}_b}. \tag{2.57}$$

Optimal Number of Sub-blocks Number of sub-blocks to be used in the transmitted block is a parameter to be determined. Number of sub-blocks means how often the training sub-blocks are inserted. Using more sub-blocks than needed causes waste of channel capacity. However, use of less sub-blocks than needed causes more error in the channel estimation.

In [18], the optimal number of sub-blocks is found by maximizing the lower bound on average channel capacity. The number of sub-blocks which maximizes the lower bound on average channel capacity is found to be

$$N_{sub} = Q + 1. \tag{2.58}$$

Optimal Power Allocation In [18] the relation between the total power transmitted, power transmitted for information symbols, and the power transmitted for training symbols is given as

$$P = P_s + P_b \tag{2.59}$$

where P_s is the power transmitted for information symbols and P_b is the power transmitted for training symbols. Also P_s is defined as [18]

$$P_s := \alpha P. \tag{2.60}$$

The optimal power allocation problem is reduced to find α. In [18] it is desired to find α such that it does not depend on channel. So, optimum α value is evaluated for three conditions in [18]. These conditions are:

1. Low SNR;
2. High SNR;
3. Identical distributed channel taps.

The optimal value of α for these conditions is found to be as

Case1) Low SNR:

$$\alpha_{low} = \frac{1}{2} \tag{2.61}$$

Case2) High SNR:

$$\alpha_{high} = \frac{1 - \left(\frac{L+1}{N_s} + \frac{(L+1)(Q+1)\sigma_\omega^2}{P}\left(1 - \frac{L+1}{N_s}\right)\right)^{1/2}}{1 - \frac{L+1}{N_s}} \tag{2.62}$$

For $SNR \to \infty$ (2.62) can be rewritten as

$$\alpha_{high} = \frac{1}{(1 + \sqrt{((L+1))/\bar{N}_s})} \tag{2.63}$$

Case3) Identical Distributed Channel Coefficients:

$$\begin{aligned} \alpha_{iid} &= \frac{\beta - \left(\beta^2 - \left(1 - \frac{L+1}{N_s}\right)\beta\right)^2}{1 - \frac{L+1}{N_s}} \\ \beta &= 1 + (L+1)(Q+1)\sigma_\omega^2/P. \end{aligned} \tag{2.64}$$

where N_s is the length of information sub-blocks.

In [18], the following table is given in order to summarize the optimal training parameter. Optimal α is given when $SNR \to \infty$.

The general structure of transmitted block is shown in Figure 2.4.

Table 2.1: Optimal parameters for training based channel estimation

Parameters	Optimal training
Placement of information symbols	Equally long information sub-blocks (length N_s)
Placement of training symbols	Equally long training sub-blocks (length N_b)
Structure of training sub-blocks	$b_p = \left[0_L^T b 0_L^T\right]^T, \forall p$
Number of training symbols	$N_b = 2L + 1$ per sub-block
Number of sub-blocks	$Q + 1$ training and $Q + 1$ information sub-blocks
Power allocation	$\alpha_{high} = \frac{1}{(1+\sqrt{((L+1))/\bar{N}_s})}$

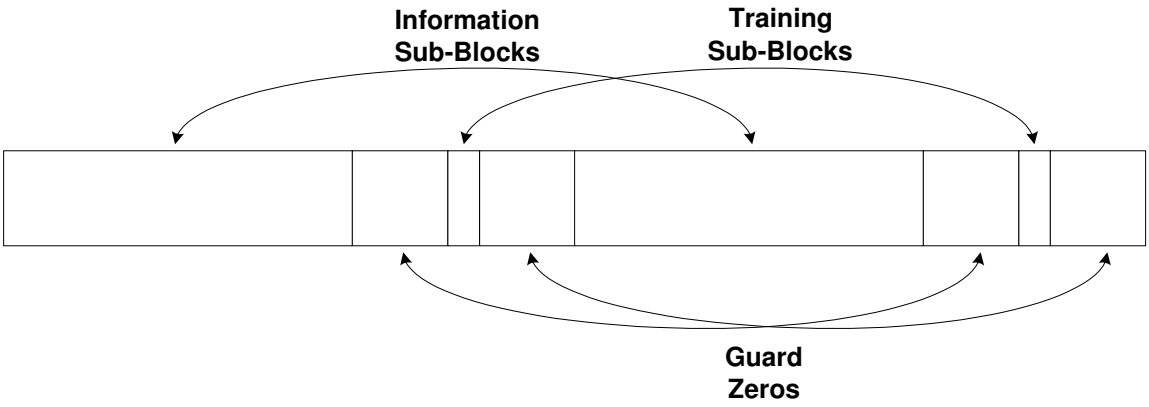

Figure 2.4: Transmitted Block

CHAPTER 3

OFDM AND SCBT

3.1 Introduction

Various researches are conducted for OFDM and SCBT and various forms of these modulation techniques are developed. In this chapter the the forms of OFDM and SCBT which are used in this thesis is described. Also the general structure and concept behind OFDM and SCBT is given.

3.2 Orthogonal Frequency Division Multiplexing

Frequency selectivity of channels is an important problem for high data rate systems. When the frequency bandwidth of the transmitted symbols exceeds the coherence bandwidth of the channel, frequency selectivity occurs. Due to frequency selectivity different frequency components of the transmitted signal experiences different gains. This fact causes heavy distortions on the received signal by the receiver. In order to combat the effects of frequency selectivity complex equalizer structures are needed in the receiver.

Orthogonal frequency division multiplexing (OFDM) is a very popular modulation technique for high data rate systems. Its popularity is based on its suitability for multipath fading channels. Negative effects of a multipath fading channel on the transmitted signal can be repaired with simple equalizer structures in an OFDM system.

History of OFDM goes back to 1960s. Since 1960s frequency division multiplexing (FDM) systems have been employed in military applications [20]. OFDM, which employs multiple carriers overlapping in the frequency domain, was pioneered by R.W. Chang in 1966 [20]. Use of DFT operation in OFDM signal generation is an important improvement for OFDM. With this technique, implementation complexity of an OFDM system reduced substantially. For today's high data rate digital systems OFDM becomes a modulation standard.

3.2.1 Qualitative Description of OFDM

In a single carrier system, data is transmitted using one carrier. A typical spectrum of a single carrier system and the spectrum of a rayleigh fading frequency selective channel are shown in Figure 3.1. In a single carrier system as data rate increases the duration of the transmitted signal reduces, the bandwidth of the signal increases. With increasing bandwidth, effects of frequency selectivity on the transmitted signal increases. So single carrier systems are more susceptible to frequency selectivity when they carry high data rates.

The concept of frequency division multiplexing (FDM) is to transmit data with multiple subcarriers instead of a single carrier [21]. So the total data rate is divided among subcarriers. A subcarrier carries information with lower rate and lower bandwidth. A typical spectrum of an FDM system and the spectrum of a rayleigh fading frequency selective channel are shown in Figure 3.2.

To prevent interference between two neighboring subcarriers, guard bands are required in FDM systems. Guard bands are considered as waste of spectrum and reduces information rate of the system compared to a single carrier system [21].

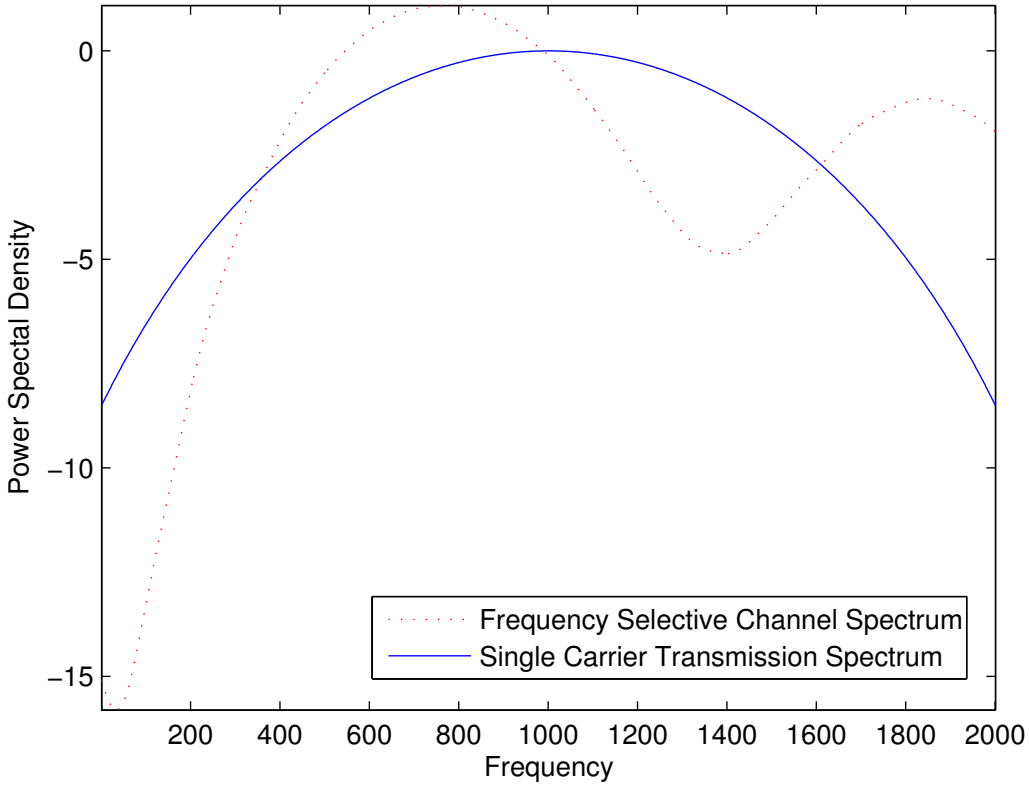

Figure 3.1: Spectrum of Single Carrier System

Orthogonal frequency division multiplexing (OFDM) can be considered as a special type of FDM with no guard bands and overlapping subchannels. A typical spectrum of an OFDM system and the spectrum of a rayleigh fading frequency selective channel are shown in Figure 3.3. Comparing the spectrum of FDM shown in Figure 3.2 with the spectrum of OFDM shown in Figure 3.3 the spectral efficiency of OFDM over FDM is obvious. The interference between overlapping subcarriers can be avoided with choosing the carriers to be orthogonal to each other. Correlation of two orthogonal stochastic processes is zero, so they are uncorrelated. A matched filter in the

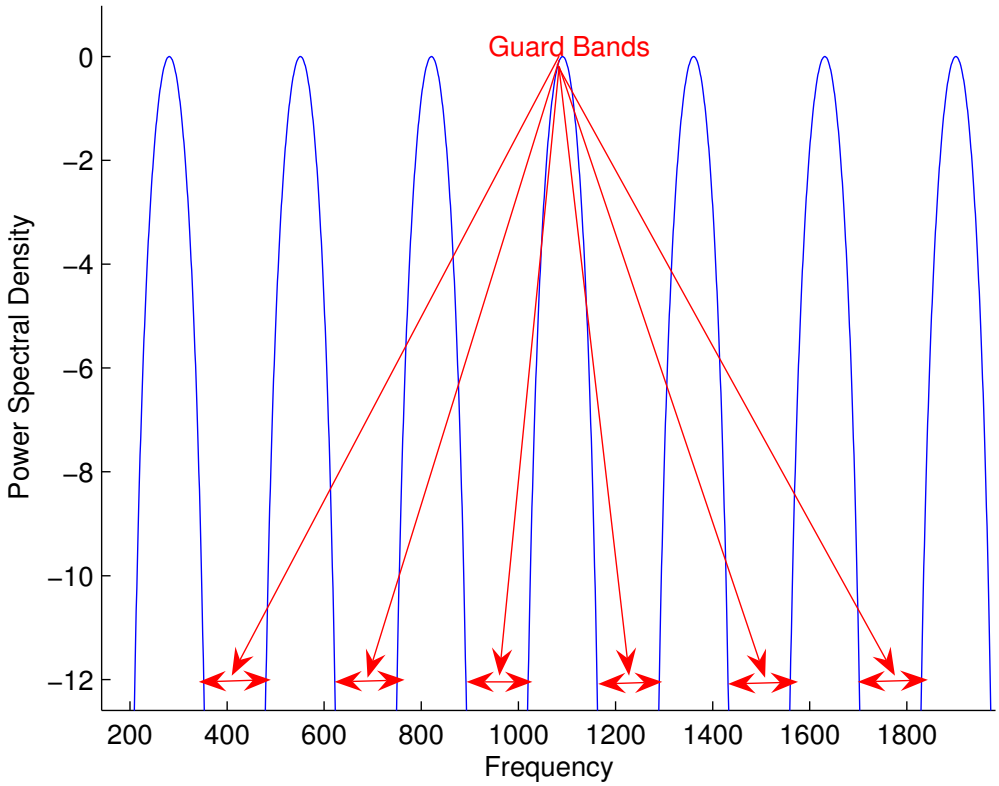

Figure 3.2: Spectrum of Frequency Division Multiplexing

receiver can be considered as a correlator. Since the correlation of different subcarriers in OFDM is zero, there will be no interference between subcarriers at the matched filters outputs in the receiver.

3.2.2 Mathematical Description of OFDM

In previous sections it is described that OFDM is basically an FDM system whose subcarrier frequencies are chosen such that these subcarriers are overlapping in frequency domain. So, in order to express OFDM mathemat-

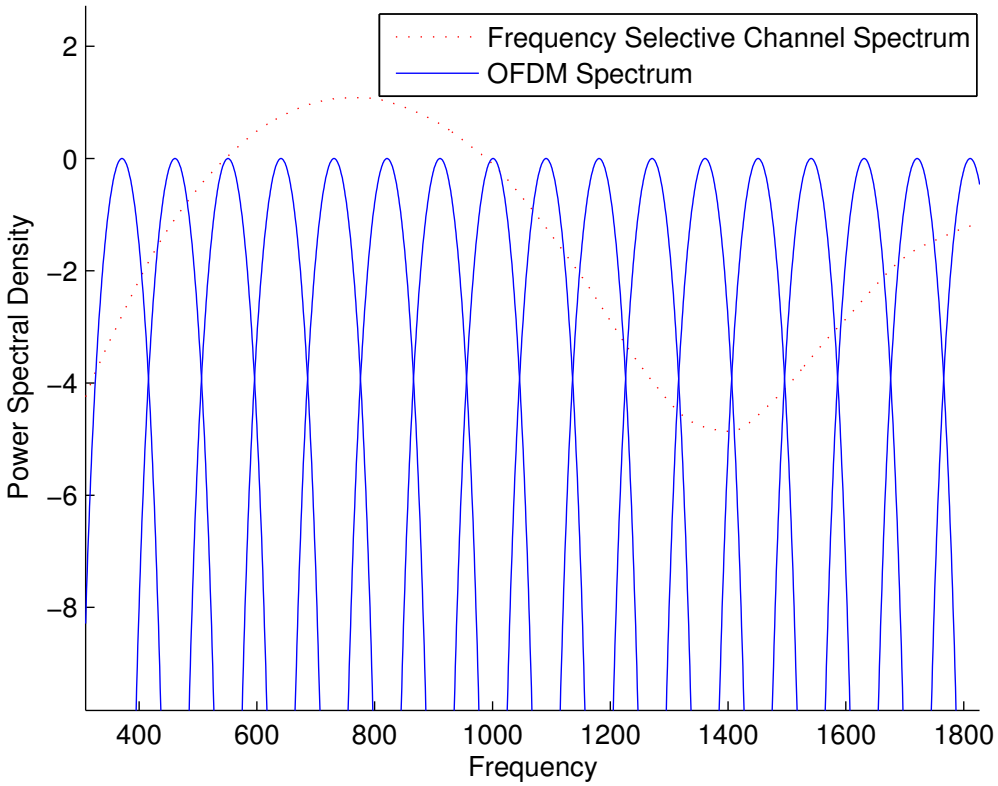

Figure 3.3: Spectrum of An OFDM System

ically it will be useful to express one subcarrier first.

Each carrier forming OFDM signal can be described as a complex wave [21]

$$s_c(t) = A_c(t)e^{j[\omega_c t + \phi_c(t)]} \tag{3.1}$$

where ω_c, $A_c(t)$, and $\phi_c(t)$ are the frequency, amplitude, and phase of the carrier, respectively.

OFDM signal is formed by summing N carriers. So OFDM signal can be

written as

$$s_s(t) = \frac{1}{N}\sum_{n=0}^{N-1} A_n(t)e^{j[\omega_n t+\phi_n(t)]} \tag{3.2}$$

where $\omega_n = \omega_0 + n\Delta\omega$.

If the signal is considered over one symbol period amplitude and phase of the carrier take on fixed values. So, amplitude and phase of the carrier over one symbol period become

$$\begin{aligned} \phi_n(t) &= \phi_n \\ A_n(t) &= A_n. \end{aligned} \tag{3.3}$$

Sampling (3.2) in time domain with a sampling frequency of $1/T$ results in

$$s_s(kT) = \frac{1}{N}\sum_{n=0}^{N-1} A_n e^{j[(\omega_0+n\Delta\omega)kT+\phi_n]}. \tag{3.4}$$

If $\omega_0 = 0$ in (3.4), (3.4) can be written as

$$s_s(kT) = \frac{1}{N}\sum_{n=0}^{N-1} A_n e^{j\phi_n} e^{j(n\Delta\omega)kT}. \tag{3.5}$$

If the frequency separation, $\Delta\omega$, is chosen as

$$\Delta\omega = \frac{2\pi}{NT} \tag{3.6}$$

(3.5) can be written as

$$s_s(kT) = \frac{1}{N}\sum_{n=0}^{N-1} A_n e^{j\phi_n} e^{fracj2\pi nkN}. \tag{3.7}$$

The last equation, 3.7 is the inverse discrete Fourier transform (IDFT) of $A_n e^{j\phi_n}$. This fact is an important milestone for OFDM. Equation (3.7) means that there is no need to use a bank of ossicillators in the transmitter of OFDM; an IDFT operation is sufficient to produce orthogonal carriers.

3.2.3 OFDM System Model

In Figure 3.4 a simple system block diagram of an OFDM system is shown. In the model transmitter is composed of two components. The first component is IDFT block. In OFDM, data symbols determines the frequency domain characteristics of the signal to be transmitted. The signal transmission is made in time domain, so in order to transmit the signal it has to be converted from frequency domain to time domain. IDFT blocks performs the frequency domain to time domain transmission. After this transformation, guard interval is inserted to the produced time domain signal.

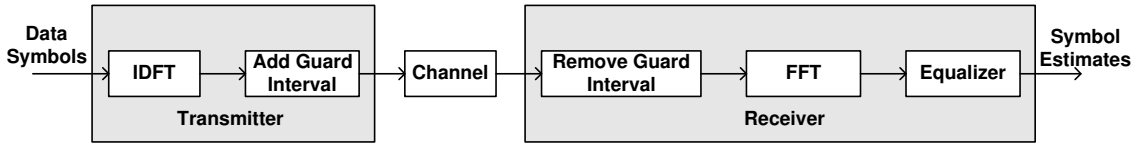

Figure 3.4: Basic OFDM System Model

Due to multipath effect in fading channels, more than one replicas of a transmitted signal arrives at the receiver at different times. This fact can cause severe problems for communications systems. As described in the previous section different symbols in an OFDM block will not interfere with each other, because the carriers of different symbols are orthogonal to each other. But different symbols with same carriers will interfere with each other. This situation can occur in a multipath environment. This fact is shown in Figure 3.5.

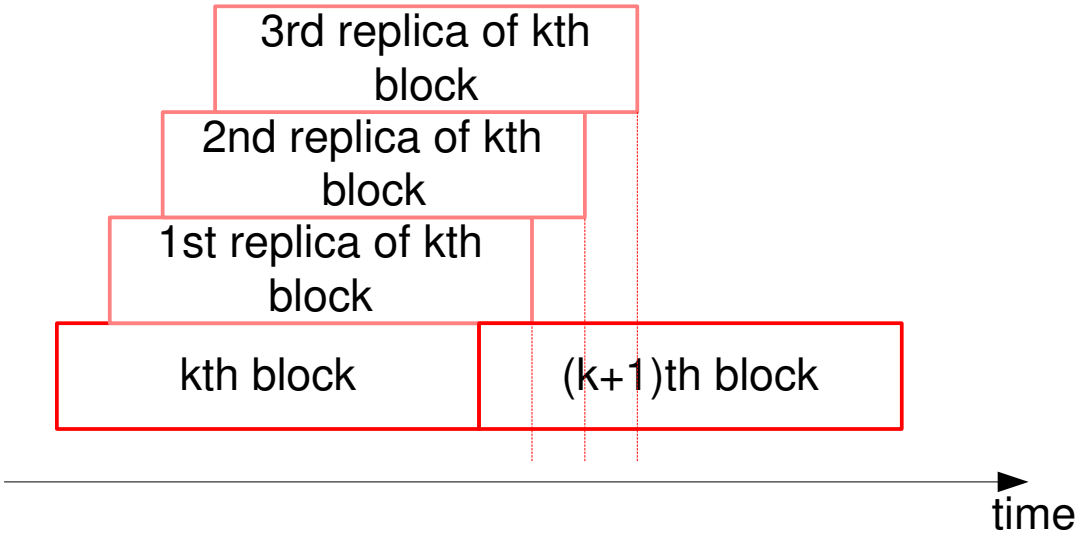

Figure 3.5: Multipath Effect in OFDM

In order to avoid overlapping of consecutive OFDM blocks resulting from multipath effect, guard intervals are used. In the literature three basic guard interval types are discussed for OFDM. These are cyclic prefix/suffix, zero padding, and known guard interval.

In cyclic prefix/suffix type guard interval the last/first L symbols of the OFDM block is inserted at the beginning/end of the OFDM block. Then, the produced block is transmitted.

Zero padding means no transmissions during guard interval. No transmissions is made either at the beginning of a block or at the end of a block.

Another type is known symbol insertion as guard interval. For this type, known symbol sequence is inserted at the beginning or at the end of the OFDM block as guard interval.

In Figure 3.7, producing cyclic prefix guard interval is shown. Also in Figure 3.8 generation of zero padding and known symbol padding type guard interval are shown.

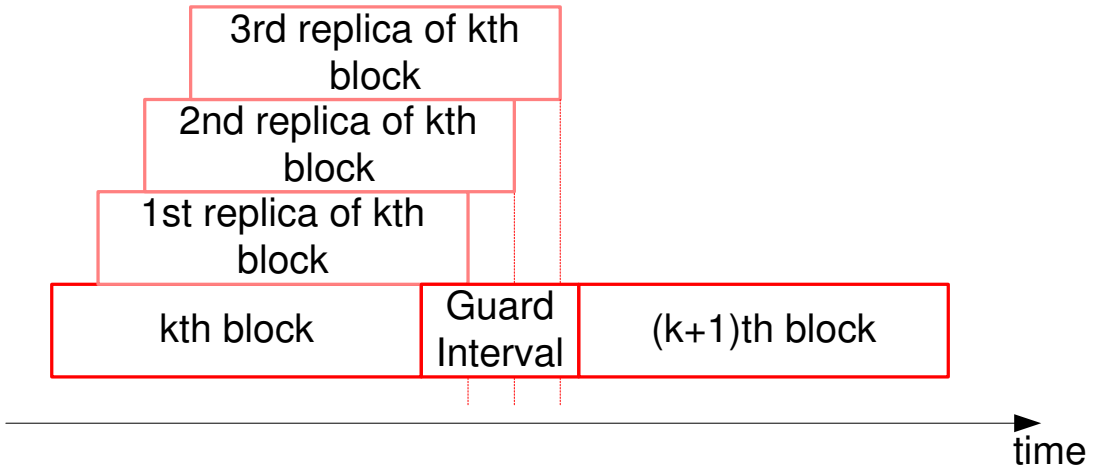

Figure 3.6: Multipath Effect in OFDM with Guard Interval

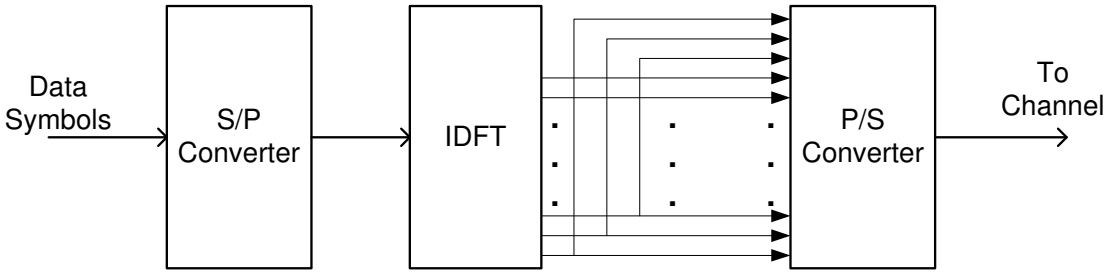

Figure 3.7: Producing Cyclic Prefix

3.2.4 Representation of OFDM With Redundant Filterbank Precoders Framework

In [1], redundant filterbank precoders representations of some modulation schemes is derived. The representation of OFDM is also presented. The transmit filters are formulated as [1]

$$f_m(n) = e^{j(2\pi/M)mn}, m \in [0, M-1], n \in [0, P-1], P = M + \bar{L} \qquad (3.8)$$

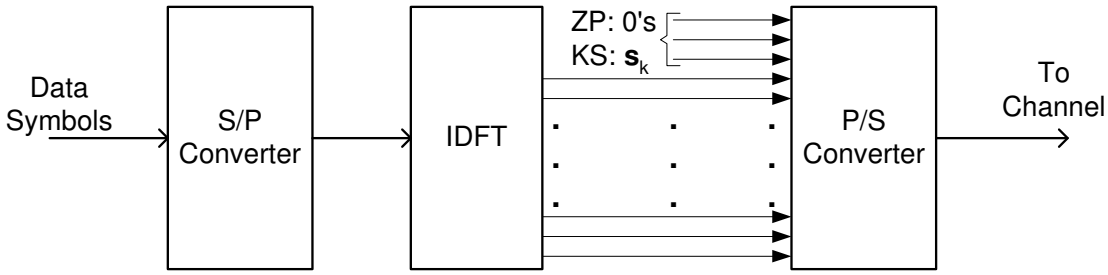

Figure 3.8: Producing Zero Padding/Known Symbol Insertion

where $\bar{L}$ is the maximum FIR channel order. This transmit filter representation corresponds to a cyclic suffix guard interval OFDM. For a zero padded OFDM system, (3.8) takes the form of

$$\begin{aligned} f_m(n) = e^{j(2\pi/M)mn}, m \in [0, M-1], n \in [0, M-1] \\ = 0, P = M + \bar{L} \end{aligned} \tag{3.9}$$

Considering (2.21), the matrix notation of the zero padded OFDM can be written as

$$\mathbf{F}_0 = \begin{pmatrix} F^H_{M\times M} \\ \mathbf{0}_{L\times M} \end{pmatrix} \tag{3.10}$$

where F^H is the $M \times M$ inverse DFT matrix and $\mathbf{0}_{L\times M}$ is the $L \times M$ matrix whose elements are 0.

Through out this thesis zero padding will be used as the guard interval for OFDM. So ZP-OFDM and OFDM will be used interchangeably.

3.3 Single Carrier Block Transmissions

Single carrier transmission, which can be considered as a traditional transmission technique,has taken attention in recent years. Single carrier modulation is considered for broadband wireless communication systems as an alternative for OFDM [10], [22].

For a conventional single carrier modulation system, equalization is a difficult task in highly dispersive channels. Since broadband wireless communication systems operate over highly dispersive channels, the equalizer structures for single carrier systems are very complex [22]. Since complexity causes high power consumption [22], this type of equalizers are not preferred especially for mobile stations due limited power capacity.

Apart from conventional single carrier modulation, block transmission (burst transmission) using single carrier is a promising modulation system for broadband systems. Block transmission reduces the equalizer complexity encountered in conventional single carrier systems. There are considerable researches on single carrier block transmissions. These researches resulted in different block structures.

3.3.1 Zero Pad Only Single Carrier Block Transmissions

In the literature the most common single carrier block transmissions schemes are cyclic prefix only (CP only) and zero pad only (ZP only). In the CP only scheme cyclic prefix is used in the guard interval. The aim of using cyclic prefix is to convert the convolution of the channel impulse response with the transmitted signal from linear convolution to circular convolution. In this way very simple frequency domain equalizer can equalize the channel effects in the receiver. In the CP only scheme, the IDFT operation in the transmitter of OFDM is transferred to the receiver.

The block structure of a CP only system is shown in Figure 3.9. Also a CP only system block diagram using a frequency domain equalizer is shown in Figure 3.10 [4].

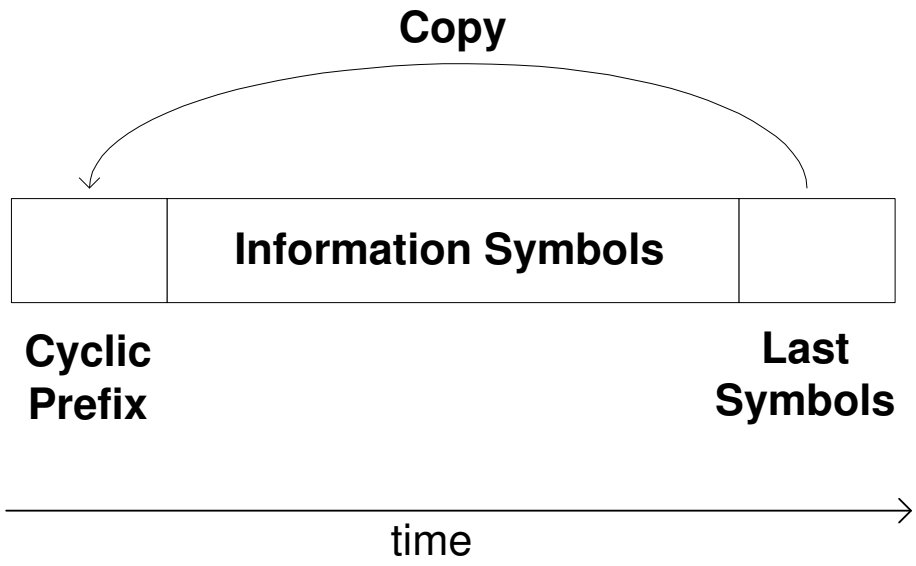

Figure 3.9: CP only block structure

In this thesis single carrier block transmissios refer to ZP only. There is considerable interest in ZP only. In [23] it was proved that ZP only achieves the maximum coding gain and maximum diversity order over rayleigh fading channels. In [3] OFDM and ZP only is compared in terms of peak-to-average power ratio, diversity order and vulnerability to frequency offset. It was also shown in [3] that ZP only can achieve the maximum diversity over rayleigh fading channels where as OFDM has the minimum diversity order over rayleigh fading channels. Also ZP only has low PAPR compared to OFDM and it is more vulnerable to frequency offset compared to OFDM. These facts make ZP only a good alternative to OFDM.

The block structure of ZP only system is shown in Figure 3.11. In this

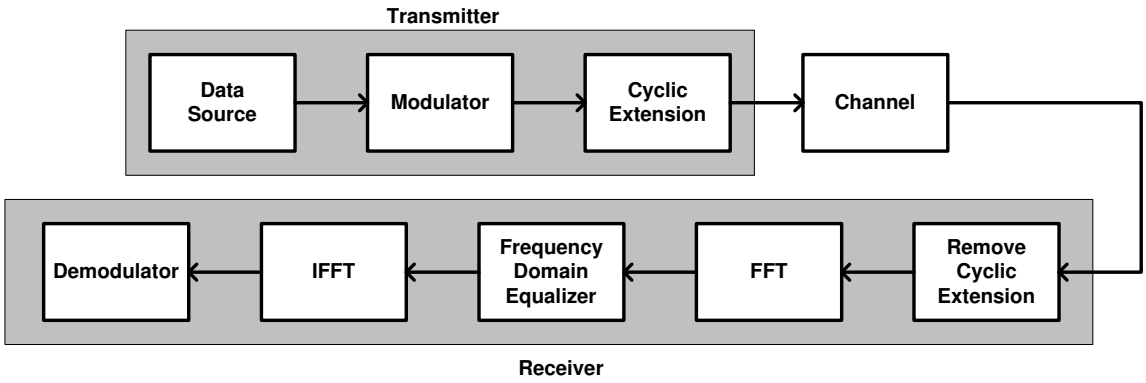

Figure 3.10: CP only block diagram

block guard interval is used as a suffix because the guard interval is after the block is transmitted. If the guard interval is used before transmitting the block then the guard interval will be called as prefix guard interval.

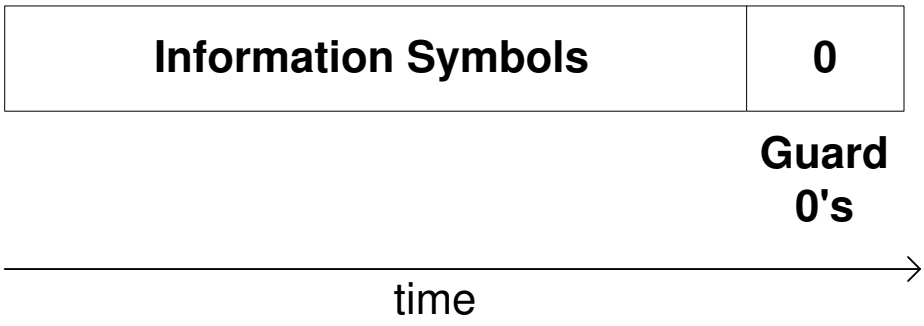

Figure 3.11: ZP only block structure

3.3.2 Redundant Filterbank Representation of ZP Only SCBT

In [3] the input-output relation of ZP only system is given as

$$\mathbf{y}(n) = \mathbf{H}\mathbf{s}(n) + \mathbf{v}(n). \tag{3.11}$$

Considering the equation (2.27), the precoder matrix for ZP only single carrier block transmissions scheme can be written as

$$\mathbf{F} = \mathbf{I}_{M\times M} \tag{3.12}$$

where $\mathbf{I}_{M\times M}$ is the the $M \times M$ identity matrix.

The precoder for ZP only can be expressed according to the equation (2.23) for a suffix guard interval as

$$\mathbf{F}_0 = \begin{pmatrix} \mathbf{I}_{M\times M} \\ \mathbf{0}_{L\times M} \end{pmatrix}. \tag{3.13}$$

chapter 4

Block Transmissions on Orthogonal Carriers

4.1 Introduction

OFDM is an effective way to cope with the frequency selectivity of the channel. Since frequency selectivity is an important problem for high speed data transmission systems, OFDM becomes very popular. OFDM also allows to design very simple equalizers. But besides these good properties of OFDM, it has some problems. In [3], the three well-known problems of OFDM are discussed. These problems are

1. The peak-to-average power ratio (PAPR) of the transmitted signal power is large, necessitating power backoff, unless PAR-reduction techniques are incorporated to control the resulting nonlinear distortion at the power-amplification stage.

2. Since information symbols are transmitted on subcarriers, OFDM is sensitive to transmit-receive oscillators' mismatch and Doppler effects, both pf which cause (sub)carrier frequency offset (CFO).

3. Uncoded OFDM does not enable the available multipath (or frequency) diversity. In fact, only diversity order one is possible through multipath Rayleigh fading channels.

In Figure 4.1 and Figure 4.2 time-frequency views of OFDM and SCBT is shown. In these figures "G.I." means guard interval.

As shown in Figure 4.1, OFDM symbols are transmitted on orthogonal carriers over a long time duration. At the end of the block a guard interval is used. In Figure 4.1 OFDM uses N orthogonal carriers. If the transmitted signal is considered in the time domain, the first one of the three well known problems of OFDM can be understood. If the signals corresponding to different carriers are in phase, they will add constructively resulting in a high amplitude signal. So the peak power of the signal becomes very large compared to its mean power. This problem is called the peak-to-average power ratio problem.

As can be seen in Figure 4.2, a data stream is transmitted using a single carrier in single carrier block transmissions scheme. After sending the data stream, a guard interval is used. If the length of the guard interval is longer than the FIR channel order, L, then the intersymbol interference occurs among symbols only located in one block. This fact allows simple equalizer design.

4.1.1 Precoder For BTOC

In Figure 4.3, time-frequency view of the proposed system, BTOC, is shown. It is obvious from Figure 4.2 that BTOC corresponds to using single carrier block transmissions on orthogonal carriers. In the system, if N equals 1 then the system becomes a single carrier block transmissions scheme. If K equals 1 then the system becomes OFDM. So, BTOC is a parametric representation which allows representing both OFDM and single carrier block transmissions.

The system model proposed in [1] will be used in this thesis to analyze BTOC. In order to use the multirate system model, first transmit filters for

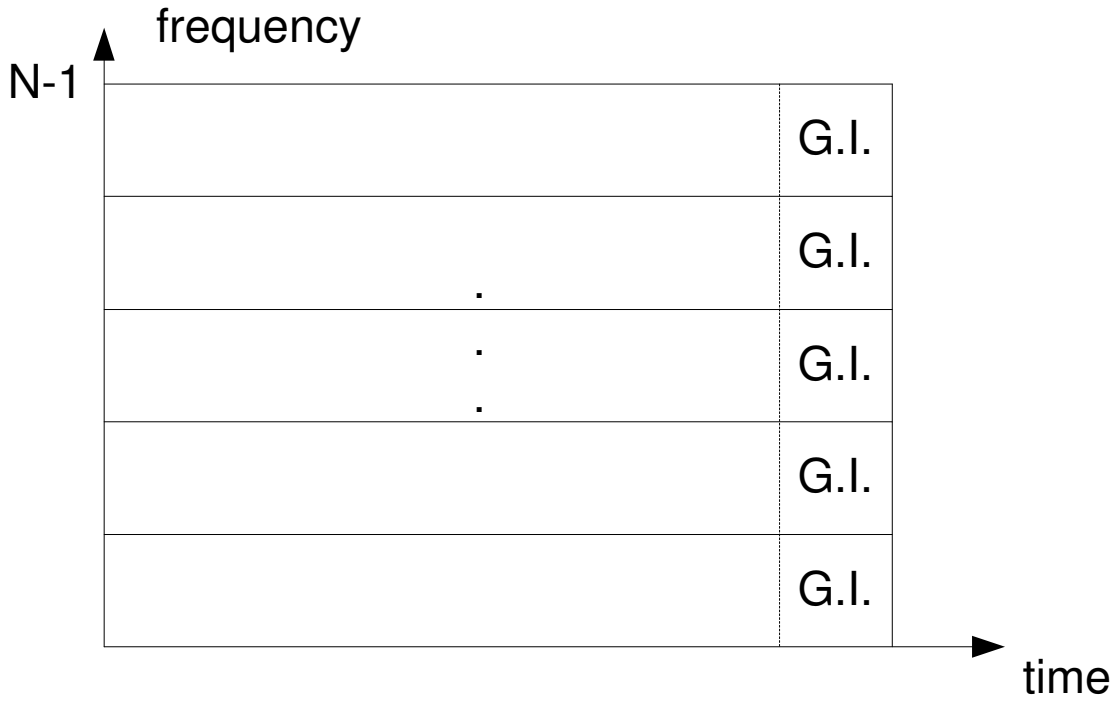

Figure 4.1: Time-frequency representation of OFDM

BTOC have to derived.

Through out this thesis zero padding is used as the guard interval for BTOC. All the derivations for BTOC will be derived for zero padding guard interval.

From 4.3 it is obvious that in BTOC, N-point IDFT of N-symbols is taken and then transmitted. This IDFT operation is repeated for K times, then a guard interval is used. So the transmit filter can be represented as

$$f_m(n) = e^{j(2\pi/N)m(n-\lfloor n/N \rfloor N)} \left[p(n - \lfloor n/N \rfloor N) - p(n - \lfloor n/N \rfloor N - N)\right] \tag{4.1}$$

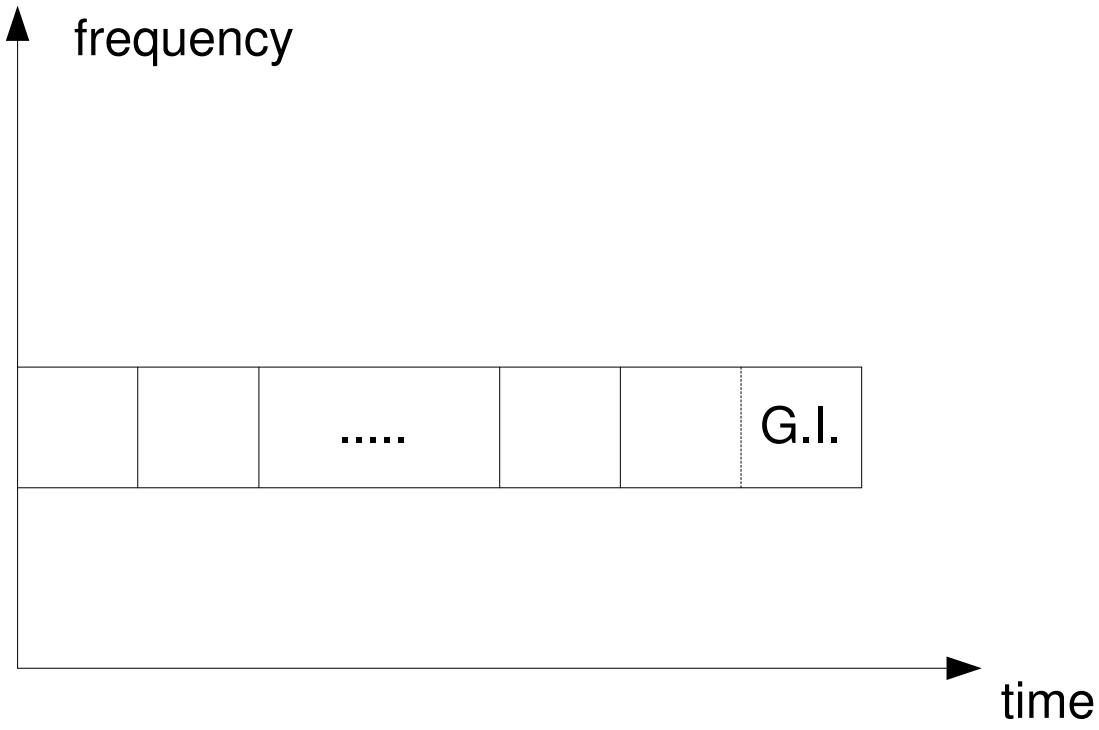

Figure 4.2: Time-frequency representation of SCBT

where $p(n)$ represents the unit step function.

So using (2.13) and (4.1) the precoder for BTOC can be formulated as

$$\mathbf{F}_0 = \begin{pmatrix} \mathbf{F}_{IDFT(0)} & \mathbf{0}_{N\times N} & \mathbf{0}_{N\times N} & \cdots & \mathbf{0}_{N\times N} \\ \mathbf{0}_{N\times N} & \mathbf{F}_{IDFT(1)} & \mathbf{0}_{N\times N} & \cdots & \mathbf{0}_{N\times N} \\ \vdots & \ddots & \ddots & \vdots & \vdots \\ \mathbf{0}_{N\times N} & \mathbf{0}_{N\times N} & \mathbf{0}_{N\times N} & \cdots & \mathbf{0}_{N\times N} \\ \mathbf{0}_{N\times N} & \mathbf{0}_{N\times N} & \mathbf{0}_{N\times N} & \cdots & \mathbf{F}_{IDFT(K-1)} \\ & & \mathbf{0}_{L\times M} & & \end{pmatrix}_{P\times M} \tag{4.2}$$

where $\mathbf{F}_{IDFT(k)}$ represents kth $N \times N$ IDFT matrix and $\mathbf{0}_{m\times n}$ represents

$m \times n$ zero matrix. Also

$$M = N \times K$$
$$P = M + L \tag{4.3}$$

holds.

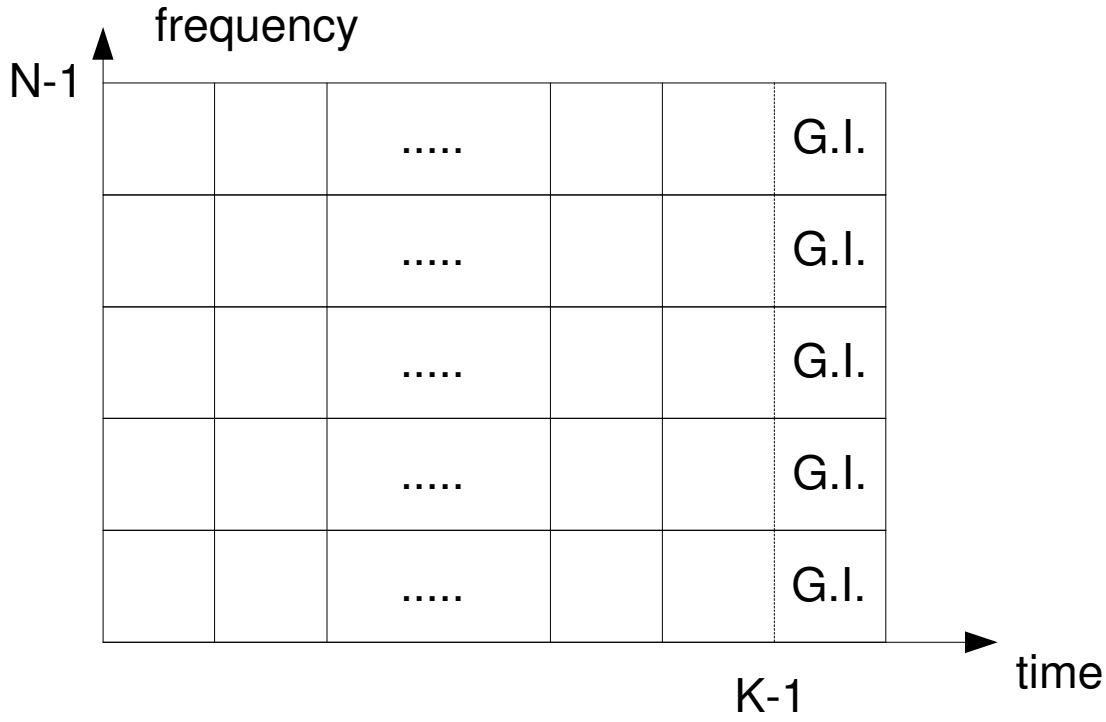

Figure 4.3: Time-frequency representation of BTOC

4.1.2 Equalizer Design For BTOC

In 2.3.1 and 2.3.2 ZF and MMSE equalizers proposed in [1] and [2] are reviewed. In the design of equalizers the first three assumptions of the four

assumptions made in 2.2 are important. In order to use the derived ZF and MMSE equalizers in a BTOC system, the system has to be checked whether it satisfies the assumption or not. Below three assumptions are checked for BTOC system:

1. This assumption does not depend on the modulation scheme. So, this assumption will hold for all modulation schemes.

2. In block transmissions on orthogonal carriers $P = N \times K + L$ and $M = N \times K$. So, the second assumption is satisfied for block transmissions on orthogonal carriers.

3. The assumption on transmit filter is satisfied as can seen from (4.1). In (4.2), it is shown that the precoder matrix of block transmissions on orthogonal carriers is a block diagonal matrix with its diagonal entries of $M \times M$ DFT matrices. Since DFT matrices are full rank and the rank of a block diagonal matrix is the sum of the ranks of its diagonal entry matrices. The rank of the precoder matrix of block transmissions on orthogonal carriers is $K \times M$, so it is full column rank. As a result the third assumption is also satisfied.

Since all the assumptions made in [1] holds for BTOC, the zf equalizer proposed in [1] and the MMSE equalizer proposed in [2] can be used for BTOC.

4.2 PAPR

A serious problem of OFDM systems is the peak-to-average power ratio problem. After transforming the frequency-domain signal to time-domain signal with IDFT at the OFDM transmitter, signals with high peak-to-average power ratio may be generated. The components used in an OFDM

system may be driven into the nonlinear operating region by this high peak power signal. So, the components in the OFDM system such as amplifier, processor, digital-to-analog converters, and analog-to-digital converters has to work in their linear operating region in a large dynamic range [7], [8]. When the transmitter is considered as a mobile station, high PAPR means short battery life. Because of these disadvantages, PAPR is an important issue in OFDM transmission.

PAPR is an important comparison factor between SCBT and OFDM. An important advantage of SCBT over OFDM is its low PAPR. So in this thesis a review of PAPR of cyclic-prefixed OFDM and SCBT will be given. Then PAPR of zero-padded OFDM and BTOC will be derived.

In [3], two PAPR definitions are given. These PAPR definitions are instantaneous PAPR and overall PAPR. The commonly used term PAPR corresponds to the overall PAPR.

The instantaneous PAPR is defined as [3]

$$PAPR_i := \frac{\| \mathbf{u}(i) \|_\infty^2}{\mathrm{E} \| \mathbf{u}(i) \|^2 / P} \tag{4.4}$$

The overall PAPR is defined as [3]

$$PAPR := \frac{max_i \| \mathbf{u}(i) \|_\infty^2}{\mathrm{E} \| \mathbf{u}(i) \|^2 / P} \tag{4.5}$$

According to (4.5), overall PAPR of cyclic-prefixed OFDM and SCBT are given in [3] as

$$PAPR^{cp-ofdm} = \frac{NA_{max}^2}{\sigma_u^2} \tag{4.6}$$

$$PAPR^{scbt} = \frac{PA_{max}^2}{M\sigma_u^2} \tag{4.7}$$

respectively. A_{max} is the amplitude of the symbol with maximum amplitude. σ_u^2 is the average energy per symbol.

Considering (4.5) and the derivation of (4.6) given in [3], the numerator of (4.5) is same for cyclic-prefixed OFDM and zero-padded OFDM. Since $P-M$ symbols of zero-padded OFDM are zero, average power of zero-padded OFDM is less than cyclic-prefixed OFDM (CP-OFDM). For zero-padded OFDM E $\parallel \mathbf{u}(i) \parallel^2 = M\sigma_u^2$. So PAPR of zero-padded OFDM is

$$PAPR^{zp-ofdm} = \frac{NA_{max}^2}{M\sigma_u^2/P} = \frac{PNA_{max}^2}{M\sigma_u^2}. \tag{4.8}$$

Since for OFDM $M = N$, (4.8) becomes

$$PAPR^{zp-ofdm} = \frac{NA_{max}^2}{M\sigma_u^2/P} = \frac{PA_{max}^2}{\sigma_u^2}. \tag{4.9}$$

To begin computing PAPR of BTOC, first the numerator of (4.5) will be considered for BTOC. BTOC transmits symbols using N carriers. After transmission of N symbols another N symbols are transmitted with using no guard interval. So the peak power at the output of the BTOC transmitter equals the peak power of OFDM. So, the numerator of (4.5) equals NA_{max}^2 for BTOC. The denominator of (4.5), mean power of a transmitted symbol is $NK\sigma_u^2/P$. So, PAPR of BTOC is

$$PAPR^{btoc} = \frac{NA_{max}^2}{NK\sigma_u^2/P} = \frac{PA_{max}^2}{K\sigma_u^2}. \tag{4.10}$$

Zero padded OFDM can modeled using the BTOC model with $K = 1$. So PAPR formulation of BTOC has to be equal to that of zero padded OFDM for $K = 1$. (4.10) for $K = 1$ equals (4.9). Zero padded SCBT is a special form of BTOC with $N = 1$. So for $N = 1$, PAPR of zero padded SCBT and PAPR of BTOC has to be equal. For $N = 1$, (4.10) is equal to (4.7).

In Figure 4.4, PAPRs of ZP-OFDM, CP-OFDM and SCBT are shown as a function of number of symbols transmitted block in a block. PAPR of BTOC as a function of number of carriers and number of serially transmitted symbols is shown in Figure 4.5.

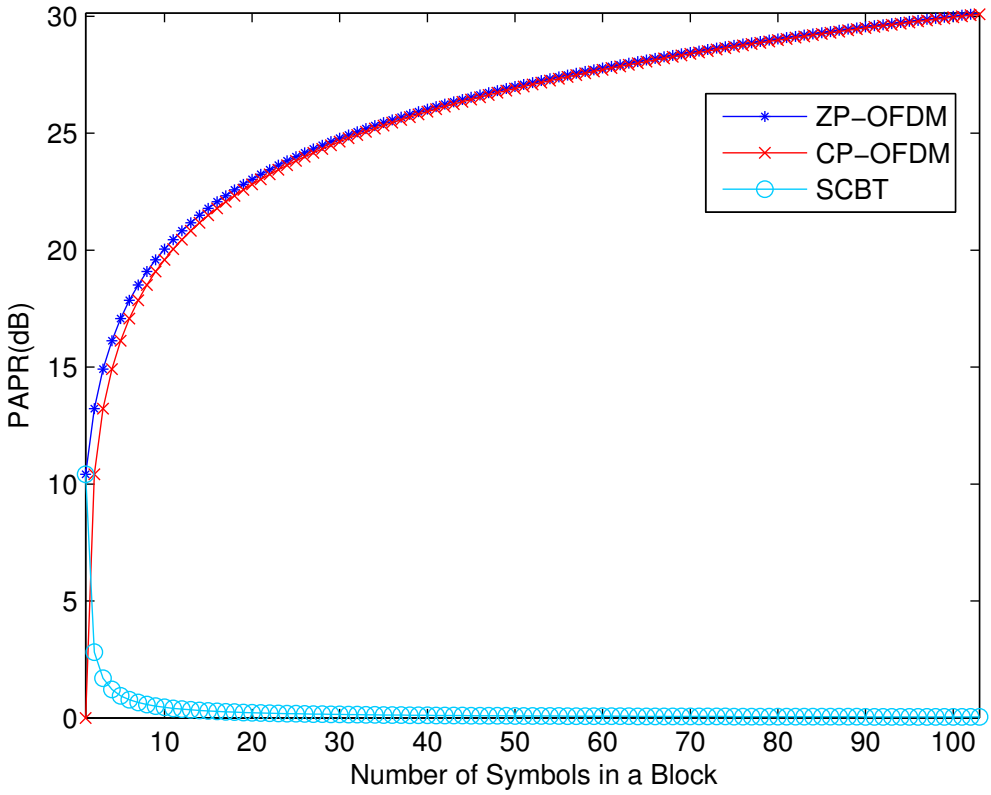

Figure 4.4: PAPR vs. number of transmitted symbols in a block for ZP-OFDM, CP-OFDM and SCBT

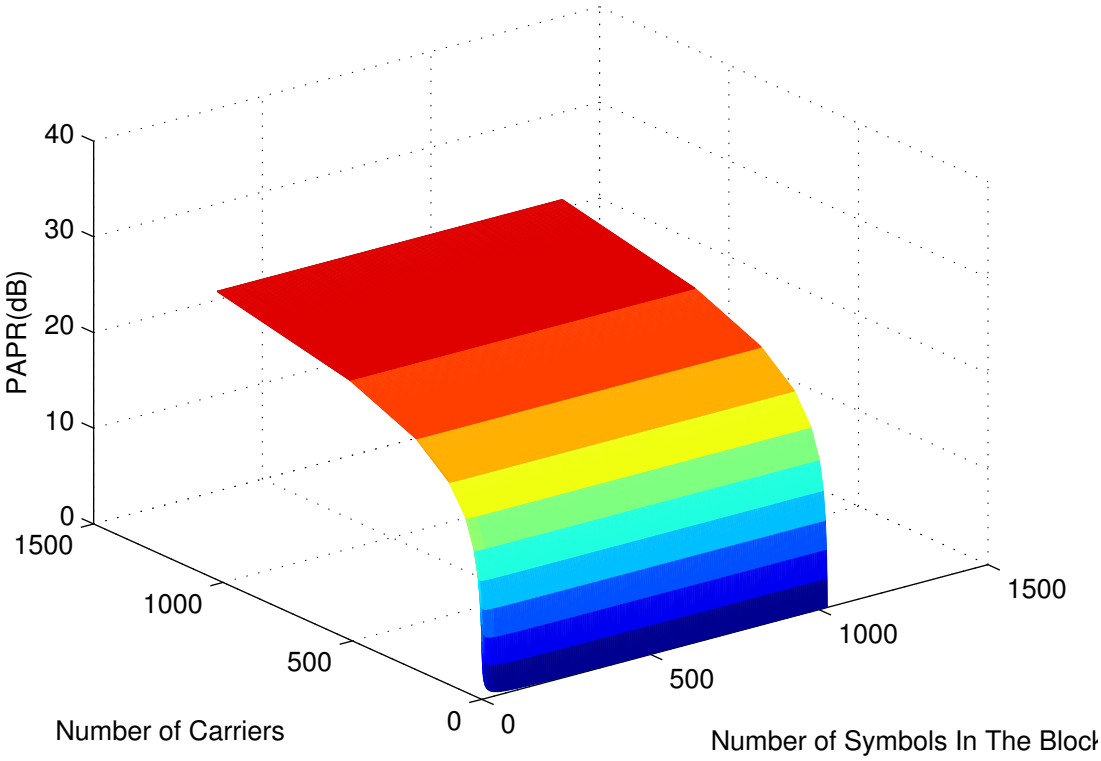

Figure 4.5: PAPR vs. number of sysmbols and number of serially transmitted symbols for BTOC

4.3 Sensitivity Of BTOC To Carrier Frequency Offset

The orthogonality of the carriers in an OFDM system allows using spectrally overlapped waveforms, thus spectrum economy is accomplished. Carrier frequency offset(CFO) between the transmitter and the receiver causes loss of orthogonality of the carriers. The loss of orthogonality can be considered as degradation of SNR of the system. In [24] the degradation in SNR

caused by CFO of an OFDM system is investigated for AWGN channel. In [3] sensitivity to CFO of OFDM and SCBT are compared.

As stated above, in [24] the channel is assumed to be AWGN. So there is no interblock interference in the considered system. Detection in the receiver is made with FFT. Also no guard interval is considered.

The degradation in SNR due to CFO is formulated in [24] as

$$D = -10 \log E_0^2 + 10 \log(1 + V_0 \frac{E_s}{N_0}). \tag{4.11}$$

In (4.11), E_0 is the useful symbol component, so E_0^2 is the power of the useful symbol component. N_0/E_s is SNR. Noise is the thermal noise. V_0 is the variance of noise components other than the thermal noise. The other noise components include intercarrier interference.

The equation (4.11), derived for the degradation in SNR due to CFO can be written approximately as

$$D \approx \frac{10}{\ln 10}((1 - E_0^2) + V_0 \frac{E_s}{N_0}) \tag{4.12}$$

when the carrier phase impairments are small [24].

Using (4.12), approximate formulas for OFDM and single carrier systems are derived.

For OFDM, the first term in (4.12) is neglected. Because the second term in the equation is the dominant term.

For single carrier communications the second term in (4.12) is zero. Because there is no intercarrier interference.

So, SNR degradation due to CFO for OFDM and single carrier systems are given in equations (4.13) and (4.14), respectively.

$$D_{OFDM} \approx \frac{10}{ln10} \frac{1}{3} (\pi N \frac{\Delta F}{R})^2 \frac{E_s}{N_0} \tag{4.13}$$

$$D_{SCBT} \approx \frac{10}{ln10}\frac{1}{3}(\pi\frac{\Delta F}{R})^2 \tag{4.14}$$

where ΔF is the frequency offset between the transmitter and the receiver, R is the symbol rate. For OFDM, $R = N/T$ and for single carrier systems, $R = 1/T$.

In [3], the formula derived for single carrier systems, (4.14), is also used for SCBT.

BTOC is a parametric transmission scheme such that it can become OFDM with suitable parameters or it can also become SCBT with other suitable parameters. So the assumptions made in order to obtain the equations (4.13) and (4.14) are not valid for BTOC. For the calculations of BTOC, equation (4.12) can be used.

In [24] V_0 is given as

$$V_0 = E[\mid \delta^2 \mid] + \sum_{m=0,m\neq k}^{N-1} E[\mid I_{k-m} \mid^2] \tag{4.15}$$

where δ is the noise term when frequency offset is random and I_{k-m} is the intercarrier interference coefficients when one block of IFFT output is considered.

In [25], ICI coefficients are given as

$$I_{k-m} = \frac{sin(\pi(l+\Delta F-k))}{Nsin(\frac{\pi}{N}(l+\Delta F-k))} exp(j\pi(1-\frac{1}{N})(l+\Delta F-k)). \tag{4.16}$$

Since frequency offset is not random, the second term in (4.15) can be written as

$$\sum_{m=0,m\neq k}^{N-1} E[\mid I_{k-m} \mid^2] = \sum_{m=0,m\neq k}^{N-1} |I_{k-m}|^2 \tag{4.17}$$

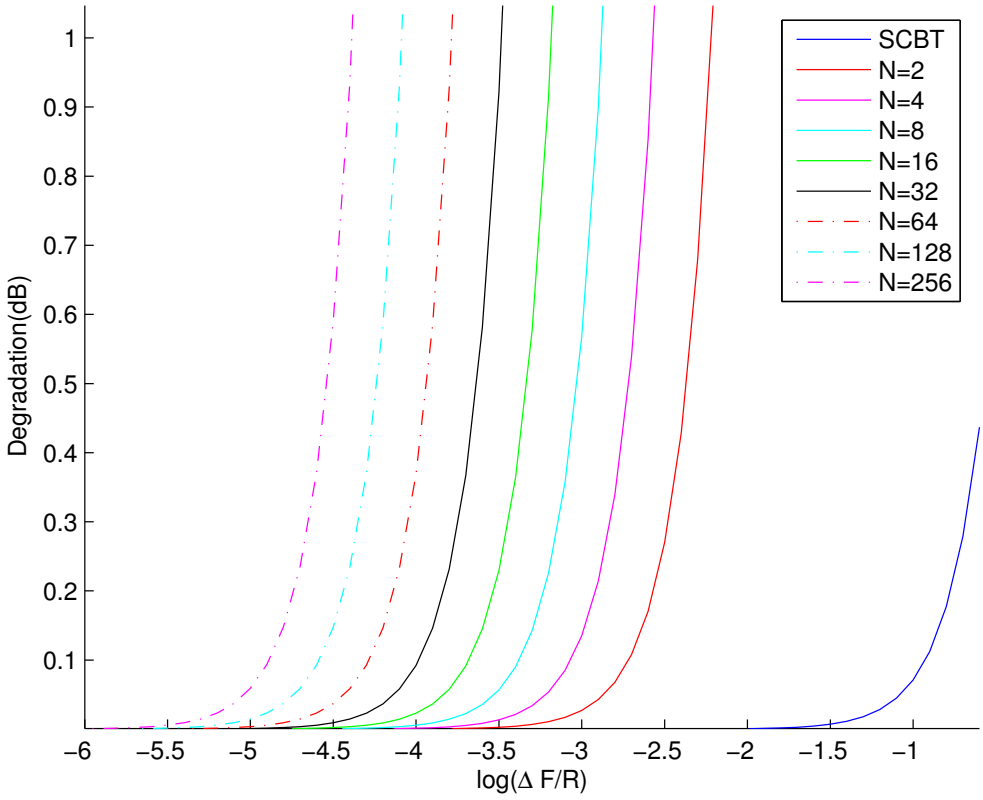

Figure 4.6: Degradation in SNR for various number of carriers.

CHAPTER 5

Simulation Results

In Chapter 4, PAPR and frequency offset sensitivity of BTOC were derived. These parameters are compared with those of ZP-OFDM and SCBT also in Chapter 4. Although PAPR and sensitivity to frequency offset are important parameters to evaluate a block transmission system, bit error rate (BER) vs. SNR performance of communication systems is the final and maybe the most commonly used comparison criterion. In this chapter, BER vs. SNR comparison of ZP-OFDM, SCBT, and BTOC is made according to the simulation results.

The simulations presented in this chapter are implemented in MATLAB. Different channel models are used in the simulations. In some simulations the channel is perfectly known by the receiver. In some simulations the channel estimation algorithms presented in Chapter 2 are used.

Both coded and uncoded performances of ZP-OFDM, SCBT, and BTOC are investigated according the to simulation results. Convolutional code and RS code are used for the systems.

One of the channel models used in [1] is an FIR channel whose order is $L = 4$ and whose zeros are located at 1, $0.9exp(j9\pi/20)$, $1.1exp(-j9\pi/20)$, and -0.8. The channel whose impulse response is

$$
\begin{aligned}
h(0) &= 1 \\
h(1) &= -0.5129 + j0.1975 \\
h(2) &= 0.2526 - j0.0395 \\
h(3) &= 0.0523 - j0.1580 \\
h(4) &= -0.7920
\end{aligned} \tag{5.1}
$$

satisfies the described channel model.

The simulation results shown in Figure 5.1 - Figure 5.10 are obtained with the channel model described above.

In the simulation results shown in Figure 5.1 and Figure 5.2 the channel is assumed to be perfectly known at the receiver. The result shown in Figure 5.1 is obtained with ZF equalizer which is formulated in (2.29). In Figure 5.2 MMSE equalizer is used instead of ZF equalizer. In both simulations each block contains 32 data symbols and 4 zeros at the end of each block as guard interval. The results are obtained for BTOC when $N = 8$ and $K = 4$.

From these results it is seen that the diversity order of SCTB is higher than both ZP-OFDM and BTOC. Because as E_b/N_0 increases BER decreases rapidly for SCBT. At low SNR, performance of three of the modulation schemes are comparable. At high SNR, effect of high diversity order of SCBT is seen. ZP-OFDM has the worst performance in these simulations. BER performance of BTOC lies between ZP-OFDM and SCBT.

In Figure 5.3 and Figure 5.4 performance of ZP-OFDM, SCBT, and BTOC with the blind channel estimation algorithm described in Chapter 2 is shown. For the result shown in Figure 5.3 ZF equalizer is used at the receiver. For the simulation whose result is shown in Figure 5.4 MMSE equalizer is used at the receiver. Compared to the previous case, the performance

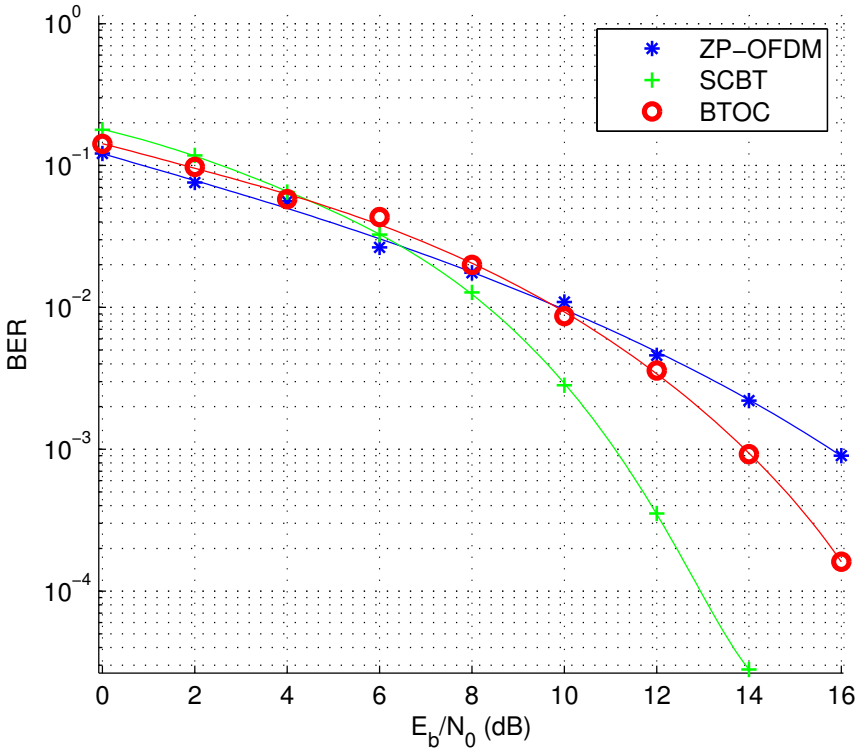

Figure 5.1: BER performance of ZP-OFDM, SCBT, and BTOC for zero-forcing equalizer(perfect channel knowledge at the receiver).

of all systems degraded slightly. But the general characteristics of the modulation schemes do not change. SCBT performs better than ZP-OFDM and BTOC, ZP-OFDM has the worst performance and the performance of BTOC lies between ZP-OFDM and SCBT as in the previous case. The parameters used for the previous case are used for these simulations.

In Figure 5.5 training based channel estimation algorithm is used instead of blind channel estimation algorithm for the system simulated in Figure 5.3 and Figure 5.4. ZP-OFDM and BTOC have very poor performance with this channel estimation algorithm. BTOC has a slightly better performance than

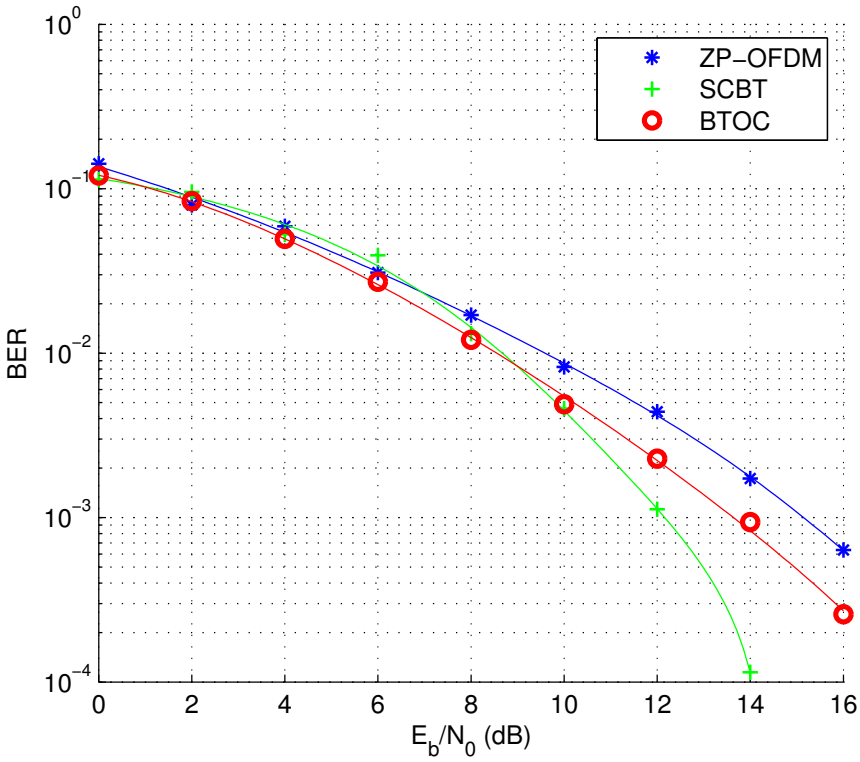

Figure 5.2: BER performance of ZP-OFDM, SCBT, and BTOC for MMSE equalizer(perfect channel knowledge at the receiver).

ZP-OFDM. The diversity order advantage of SCBT becomes obvious with increasing SNR.

For the results shown in Figure 5.1 - Figure 5.5 coding is not used at the transmitter. For the simulations whose results are shown in Figure 5.6 - Figure 5.15 different types of coding are used for different channel models and different system parameters.

In Figure 5.6 and Figure 5.7 performance of the system which is same as the system in Figure 5.1 and 5.2 are shown with convolutional coding used at the transmitter. The rate of the code is 1/2. Viterbi decoder is

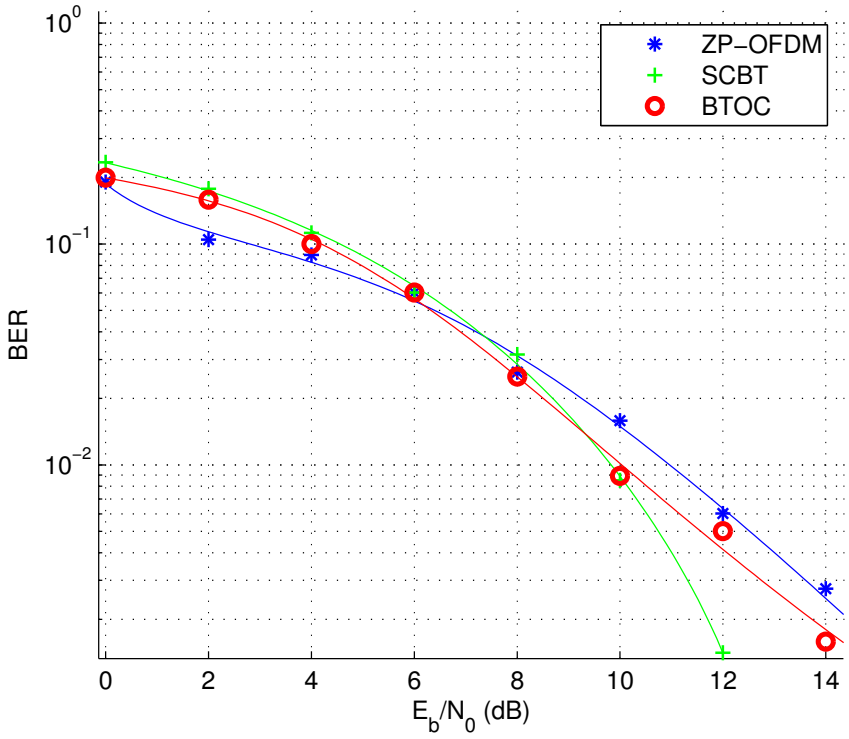

Figure 5.3: BER performance of ZP-OFDM, SCBT, and BTOC for zero-forcing equalizer(blind channel estimation).

used in the receiver. The traceback length of the Viterbi decoder is 10. It is obvious from the figures that BTOC shows the best performance among ZP-OFDM and SCBT for high SNR. In Figure 5.8 rate 3/4 convolutional code is used at the transmitter for the same system used in the previous simulation. Rate 1/2 convolutional encoder is used at the transmitter. The code is converted to rate 3/4 with puncturing. The puncturing matrix used is [111001]. Traceback length of the Viterbi decoder used in the receiver is 20. As with rate 1/2 convolutional coding with rate 3/4 BTOC also shows better performance than ZP-OFDM and SCBT.

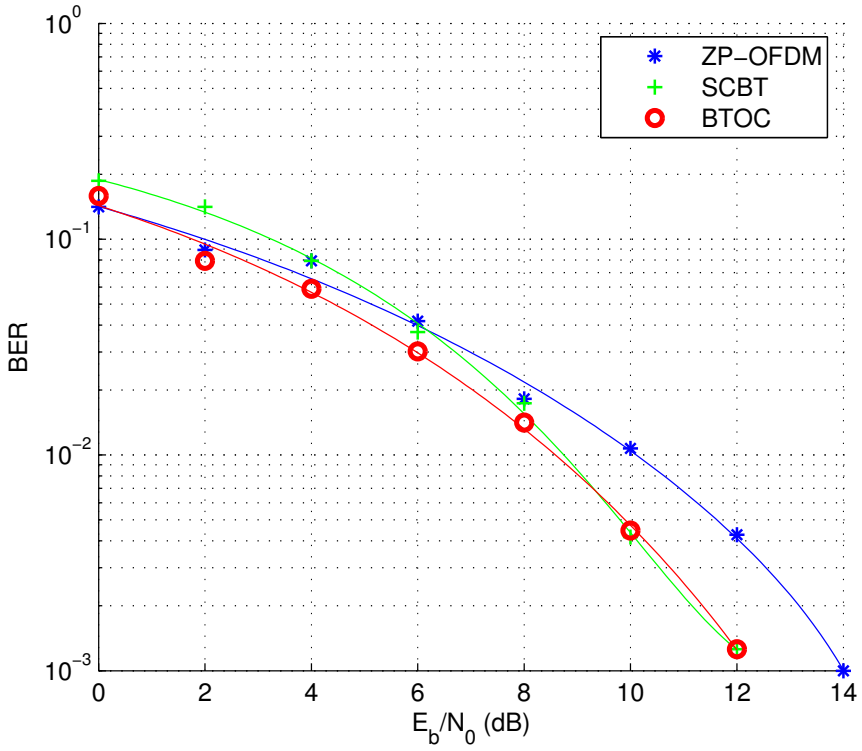

Figure 5.4: BER performance of ZP-OFDM, SCBT, and BTOC for MMSE equalizer(blind channel estimation).

Similar results are obtained with rate 1/2 convolutional encoder for the block length of 64. These results are shown in figures Figure 5.9 and Figure 5.10. For these simulations the number of carriers parameter for BTOC, N, is used as 8 and the number of serially transmitted symbols, K, is also used as 8.

In Figure 5.9 and Figure 5.10 performance of convolutionally coded ZP-OFDM, SCBT, and BTOC is shown for a block length of 64. Rate 1/2 convolutional encoder is used at the transmitter. At the receiver side Viterbi decoder is used with a traceback length of 10.

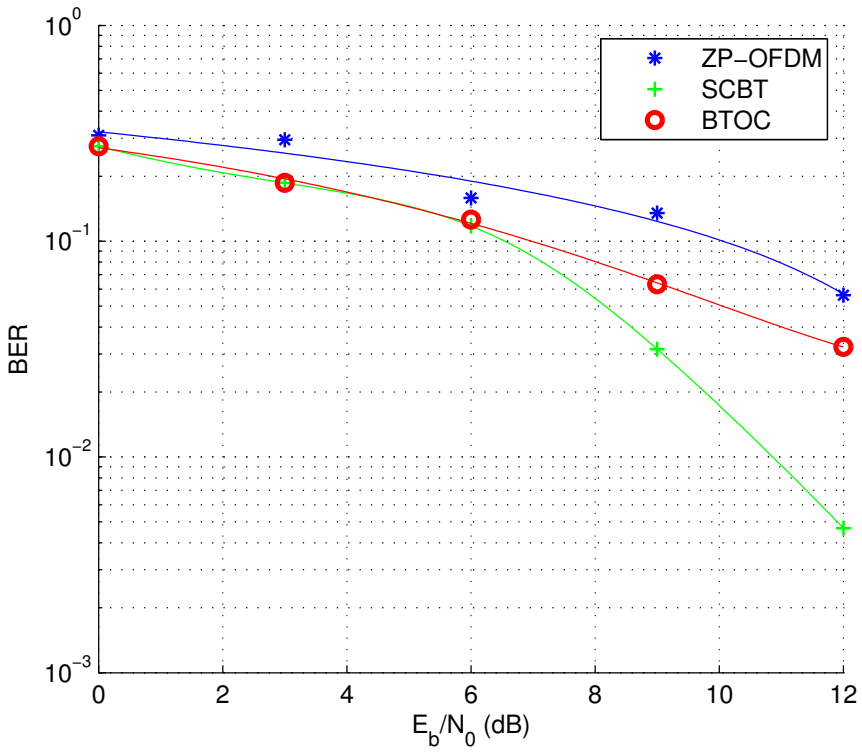

Figure 5.5: BER performance of ZP-OFDM, SCBT, and BTOC for ZF equalizer(training based channel estimation).

For the simulation results shown in Figure 5.11 - Figure 5.13 the HIPERLAN/2 channel model given in [3] is used. The results are averaged over 500 channel realizations. For the results shown in Figure 5.11 convolutional coding is used at the transmitter. At the receiver ZF equalizer is used. Each block has 64 data symbols.

In Figure 5.11 rate 1/2 convolutional encoder is used. BTOC shows the highest performance for high SNR. At low SNR ZP-OFDM is better but there is significant performance difference between ZP-OFDM and BTOC.

In Figure 5.12 rate 3/4 convolutional encoder is used. Puncturing is

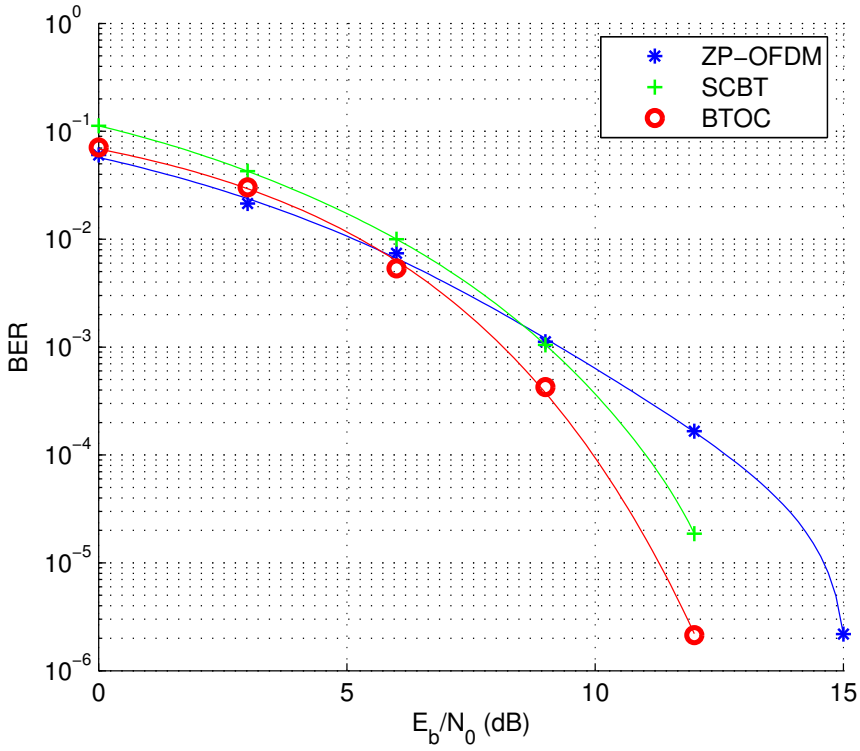

Figure 5.6: BER performance of ZP-OFDM, SCBT, and BTOC with convolutional coding (M=32, ZF equalizer, 1/2 code rate)

performed at the transmitter in order to obtain rate 3/4 code from rate 1/2 encoder. The puncturing matrix used is [111001]. In this simulation performances of BTOC and SCBT are similar. ZP-OFDM shows worse performance compared to BTOC and SCBT.

In Figure 5.13, RS encoder is used at the transmitter. In this simulation ZP-OFDM performs better that ZP-OFDM and SCBT both for low SNR and high SNR.

For the simulations whose results are shown in Figure 5.14 and Figure 5.14 a three tap channel is used. Each tap is represented by real Gaussian

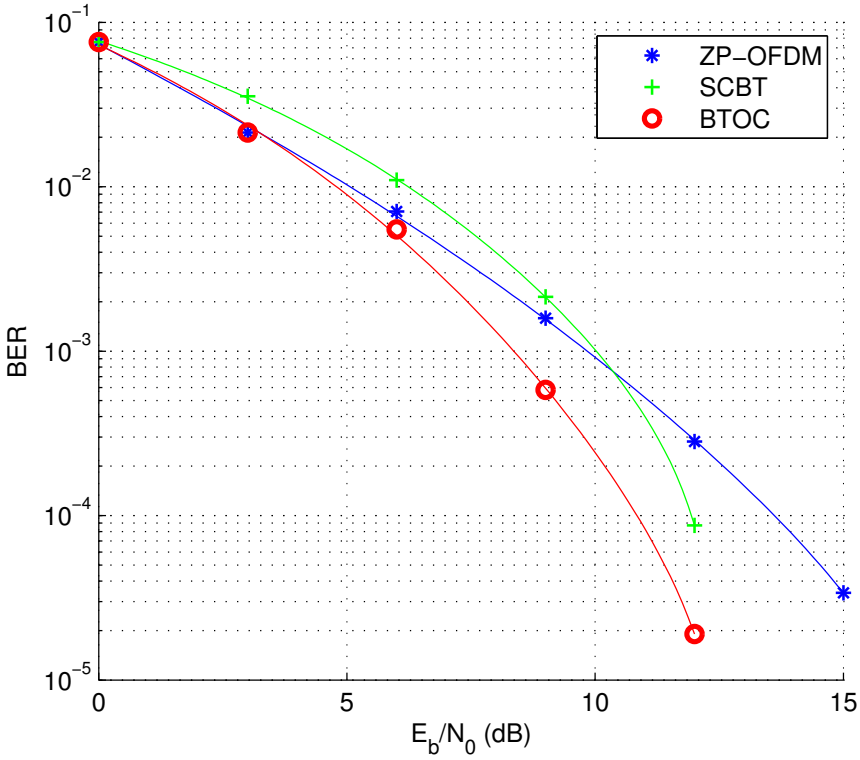

Figure 5.7: BER performance of ZP-OFDM, SCBT, and BTOC with convolutional coding (M=32, MMSE equalizer, 1/2 code rate)

random variable whose mean value is 0 and variance is 1/3.

In Figure 5.14 rate 1/2 convolutional encoder is used at the transmitter. In Figure 5.15 rate 3/4 convolutional encoder is used. For rate 1/2 performances of ZP-OFDM and BTOC are similar and better than the performance of SCBT. For rate 3/4 all of the considered modulation schemes show similar performance.

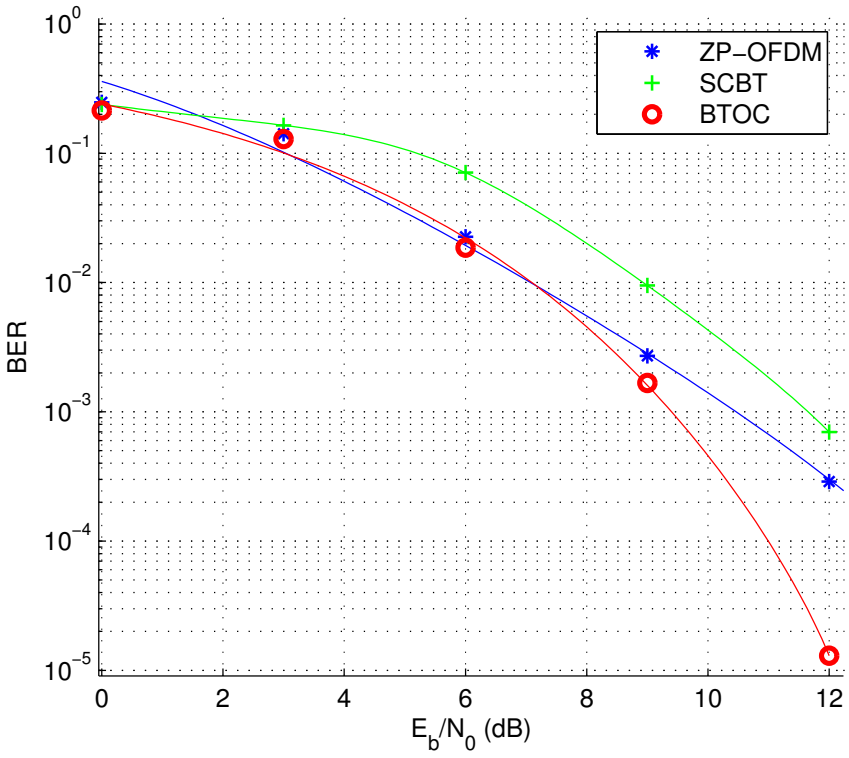

Figure 5.8: BER performance of ZP-OFDM, SCBT, and BTOC with convolutional coding of rate (M=32, ZF equalizer, 3/4 code rate)

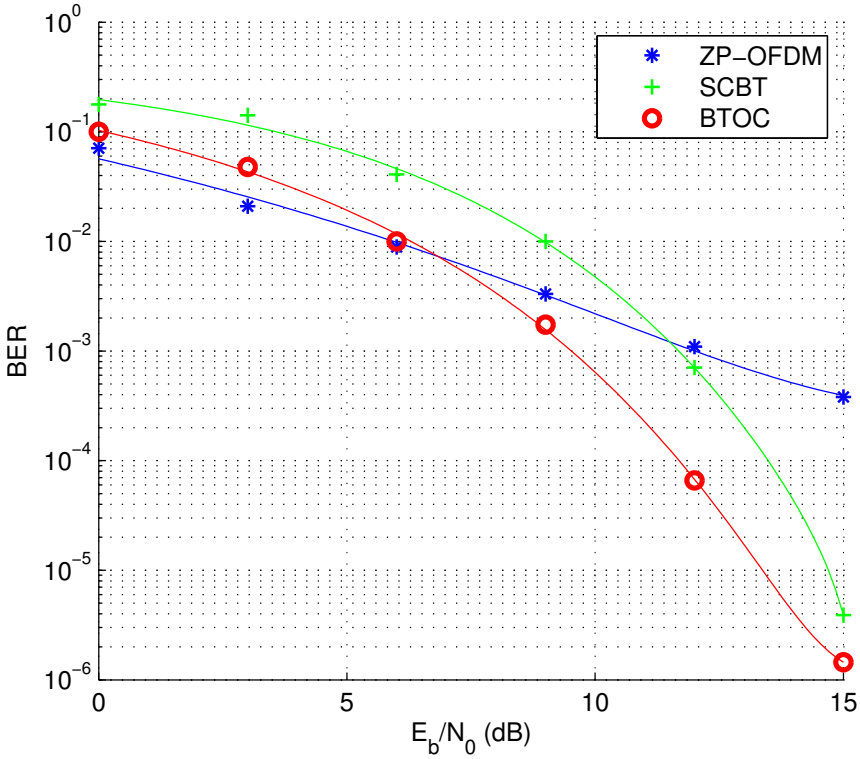

Figure 5.9: BER performance of ZP-OFDM, SCBT, and BTOC with convolutional coding (M=64, ZF equalizer, 1/2 code rate)

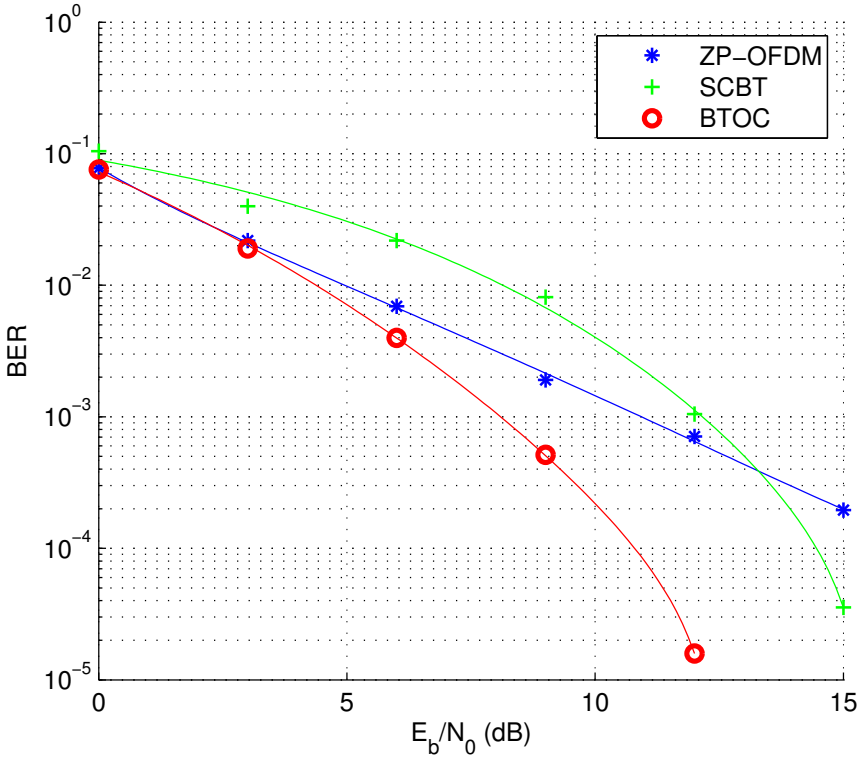

Figure 5.10: BER performance of ZP-OFDM, SCBT, and BTOC with convolutional coding (M=64, MMSE equalizer, 1/2 code rate)

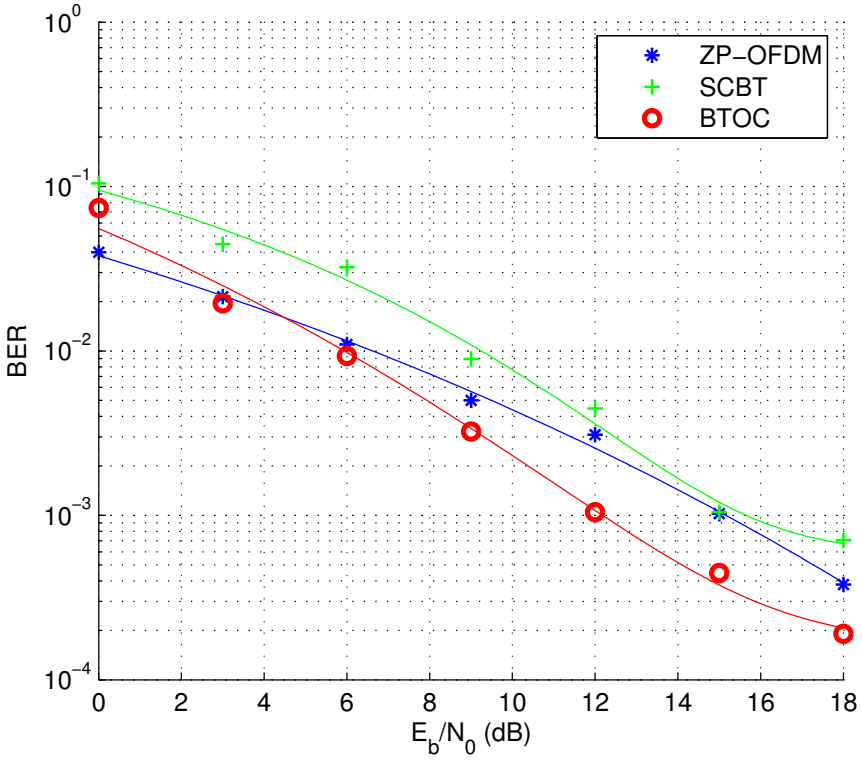

Figure 5.11: BER performance of ZP-OFDM, SCBT, and BTOC with convolutional coding on HIPERLAN/2 channel (M=64, ZF equalizer, 1/2 code rate)

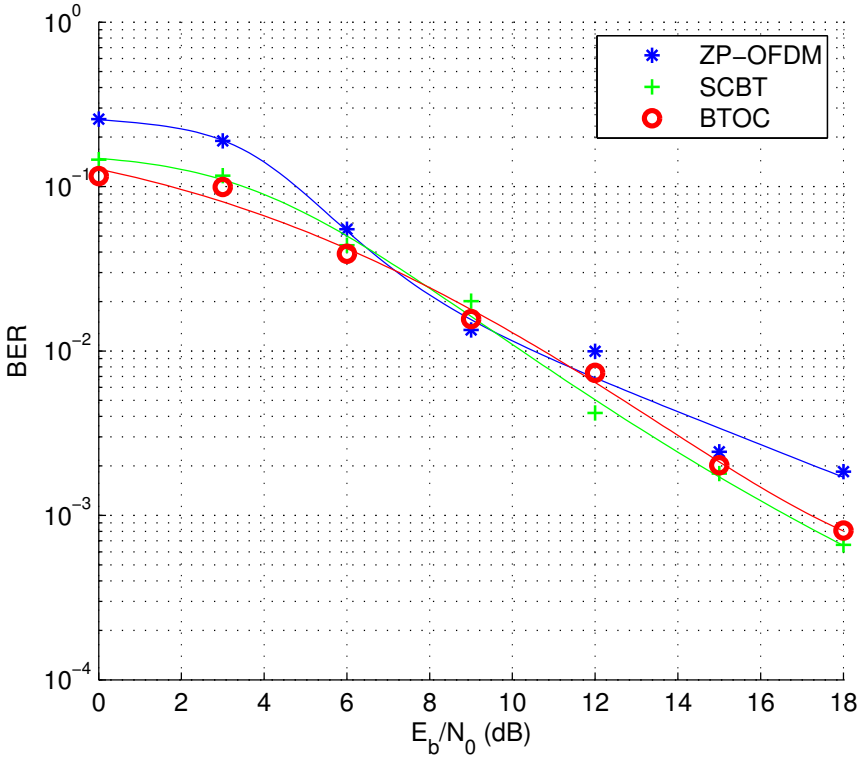

Figure 5.12: BER performance of ZP-OFDM, SCBT, and BTOC with convolutional coding on HIPERLAN/2 channel (M=32, ZF equalizer, 3/4 code rate)

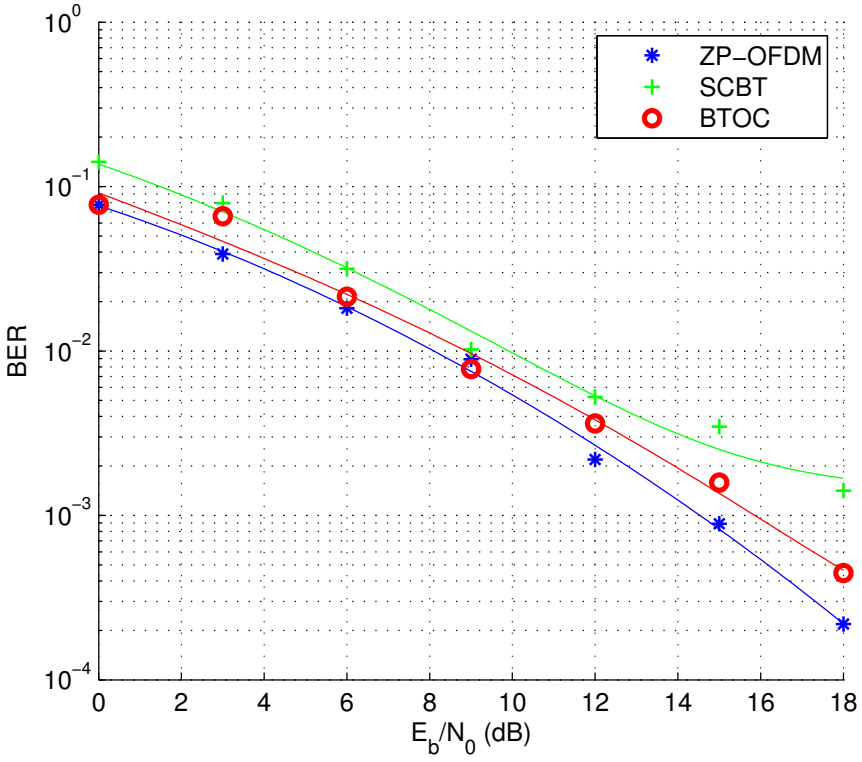

Figure 5.13: BER performance of ZP-OFDM, SCBT, and BTOC with RS coding on HIPERLAN/2 channel (M=64, ZF equalizer)

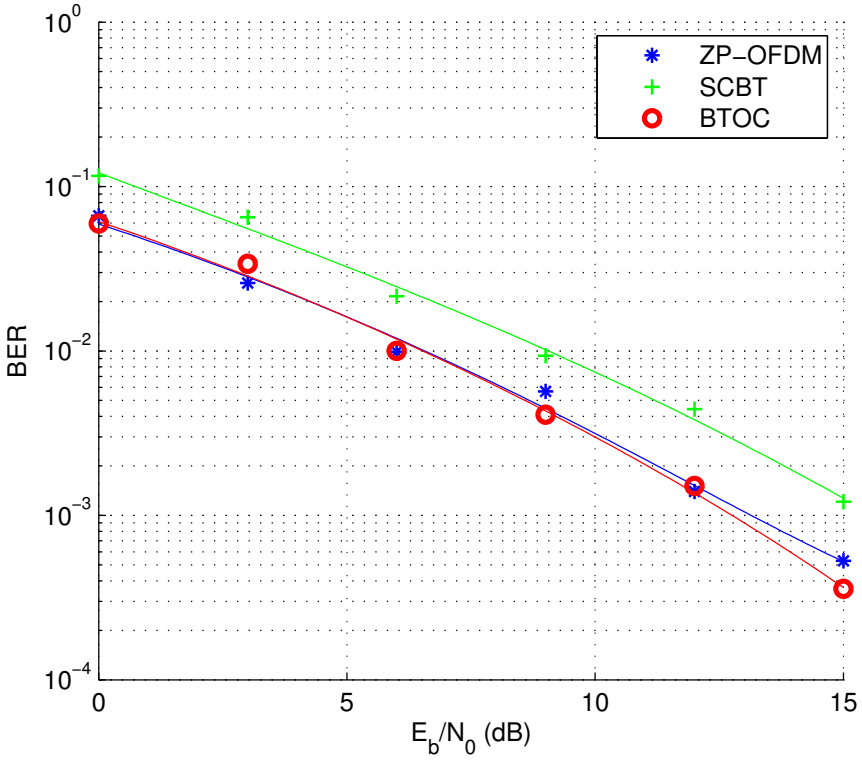

Figure 5.14: BER performance of ZP-OFDM, SCBT, and BTOC with convolutional coding on three identical tap channel (M=32, ZF equalizer, 1/2 code rate)

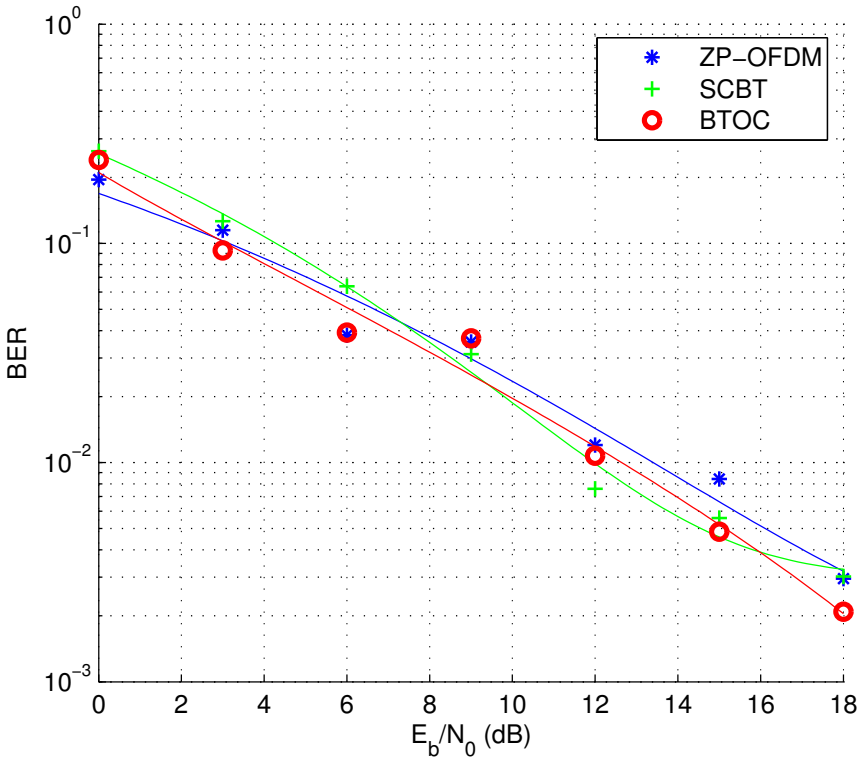

Figure 5.15: BER performance of ZP-OFDM, SCBT, and BTOC with convolutional coding on three identical tap channel (M=32, ZF equalizer, 3/4 code rate)

CHAPTER 6

Conclusions

In this thesis a new block transmissions scheme is proposed. This scheme, BTOC, can be considered as the bridge of the gap between OFDM and SCBT.

An important problem of OFDM systems is their high PAPRs. Various algorithms are developed in order to reduce the PAPR of OFDM. In order to achieve high data rates with OFDM large number of carriers are needed. With increasing number of carriers PAPR of OFDM increases. So, PAPR reduction algorithms has to be used in order to reduce PAPR in an OFDM system. The PAPR reduction algorithms brings complexity to the system. In a BTOC system same date rates with OFDM can be achieved with different number of carriers. This is accomplished with transmitting symbols on carriers serially. Reduction in number of carriers results increase in serially transmitted symbols. This structure of BTOC provides flexibility on number of carriers and PAPR.

Another important problem of OFDM systems is their vulnerability to frequency offset between the transmitter and the receiver. As in PAPR, number of carriers is an important parameter in this problem. Frequency offset between the transmitter and the receiver results in degradation in SNR of the system. Degradation in SNR means increase in BER. As the carriers increased degradation increases. Since BTOC provides flexibility on number of carriers, less degradation can be achieved with BTOC by using low number of carriers for same data rates.

Both PAPR and vulnerability to frequency offset are problems of OFDM

not SCBT. So if one only considers these problems the best modulation scheme among OFDM, SCBT, and BTOC is SCBT. SCBT has the less PAPR than PAPRs of OFDM and BTOC. Also degradation in SNR caused by frequency offset is less than the degradation in OFDM and BTOC systems. At this point BER performance as a function of SNR is an important comparison criterion.

The simulations are performed for ZP-Only as SCBT, ZP-OFDM as OFDM and BTOC. In the simulations, SCBT has the better performance than OFDM and SCBT for high SNR when coding is not used. For the uncoded case BTOC performs better than OFDM.

When RS coding is used, OFDM performs better than SCBT and BTOC.The performance of BTOC is better than the performance of SCBT with RS coding.

BTOC performs well with convolutional coding. In the simulations there is considerable difference between the performances of OFDM and SCBT compared to the performance of BTOC with convolutional coding.

REFERENCES

[1] A. Scaglione, G.B. Giannakis, S. Barbarossa, "Redundant Filterbank Precoders and Equalizers Part 1: Unification and Optimal Designs", *IEEE Trans. Signal Processing*, vol. 47, pp. 1999-2006, July 1999.

[2] A. Scaglione, G.B. Giannakis, S. Barbarossa, "Redundant Filterbank Precoders and Equalizers Part II: Blind Channel Estimation, Synchronization, and Direct Equalization", *IEEE Trans. Signal Processing*, vol. 47, pp. 2007-2022, July 1999.

[3] Zhengdao Wang, Xiaoli Ma, Georgios B. Giannakis, "OFDM or Single-Carrier Block Transmissions?", *IEEE Trans. Communications*, vol. 52, pp. 380-394, March 2004

[4] A. Czylwik, "Comparison between adaptive OFDM and single carrier modulation with frequency domain equalization" in *Proc. VTC'97*, 1997, pp. 865-869

[5] N. Benvenuto, S. Tomasin, "On the Comparison between OFDM and Single Carrier Modulation with a DFE using Frequency Domain Fedforward Filter", *IEEE Transactions on Communications*, vol. 50, pp. 947-955, June 2002.

[6] D.Falconer, S.L. Ariyavisitakul, A. Benyamin-Seeyar, B. Eidson, "Frequency Domain Equalization for Single-Carrier Broadband Wireless Systems", *IEEE Communications Magazine*, vol. 40, pp. 58-66, April 2002.

[7] Dov Wulich, Nati Dinur, and Alex Glinowiecki, "Level Clipped High-Order OFDM", *IEEE Trans. Communications*, vol. 48, pp. 928-930, June 2000.

[8] Jan Tubbax, Boris Côme, Liesbet Van der Perre, Luc Deneire, Stephane Donnay, Marc Engels, "OFDM versus Single Carrier with Cyclic Prefix: a system-based comparison", *IEEE VTS 54th Vehicular Technology Conference 2001*, pp. 1115-1119, October 2001.

[9] L. Deneire, B. Gyselinckx, and M. Engels, "Training Sequence versus Cyclic Prefix-A new look on Single Carrier Communication", *IEEE Commun. Lett.*, vol. 5, pp. 292-294, Jul. 2001.

[10] Tingting Shi, Shidong Zhou, Yan Yao, "Capacity of single carrier systems with frequency-domain equalization" in *IEEE 6th CAS Symp. on Emerging Technologies: Mobile and Wireless Comm.*, pp. 429-432, June 2004.

[11] "Single carrier and OFDM modulation their suitability for broadband fixed wireless systems", Cambridge Broadband White Paper.

[12] Anastasios Stamoulis, Georgios B. Giannakis, Anna Scaglione, "Block FIR Decision-Feedback Equalizers for Filterbank Precoded Transmissions with Blind Channel Estimation Capabilities", *IEEE Trans. Communications*, vol. 49, pp. 69-83, January 2001.

[13] Geert Leus, Marc Moonen, "Semi-Blind Channel Estimation For Block Transmissions with Non-Zero Padding" *Thirty-Fifth Asilomar Conference on Signals, Systems and Computers*, pp. 762-766, 2001.

[14] Bertrand Muquet, Shengli Zhou, Georgios B. Giannakis, "Subspace-based Estimation of Frequency-Selective Channels For Space-Time Block Precoded Systems" *Thirty-Fourth Asilomar Conference on Signals, Systems and Computers*, 2000.

[15] Tepedelenlioglu, C.; Giannakis, G.B., "Transmitter redundancy for blind estimation and equalization of time- and frequency-selective chan-

nels", *Conference Record of the Thirty-Second Asilomar Conference on Signals, Systems & Computers*, pp. 1138-1142, Nov. 1998.

[16] Shuichi Ohno, Georgios B. Giannakis, "Optimal Training and Redundant Precoding for Block Transmissions With Application to Wireless OFDM" *IEEE Trans. Communications*, vol. 50, pp. 2113-2123, December 2002.

[17] Shuichi Ohno, Georgios B. Giannakis, "Superimposed Training on Redundant Precoding for Low-Complexity Recovery of Block Transmissions" *ICC 2001 - IEEE International Conference on Communications*, pp. 1521-1525, June 2001.

[18] Xiaoli Ma, Georgios B. Giannakis, Shuichi Ohno, "Optimal Training for Block Transmissions Over Doubly Selective Wireless Fading Channels" *IEEE Trans. Signal Processing*, vol. 51, pp. 1351-1365, May 2003.

[19] Xiaoli Ma, Georgios B. Giannakis "Maximum-Diversity Transmissions over Doubly-Selective Wireless Channels" *IEEE Transactions on Information Theory*, vol. 49, pp. 1832-1840, July 2003.

[20] L. Hanzo, C. H. Wong, M. S. Yee, *Adaptive Wireless Transceivers*, Baffins Lane, Chichester, West Sussex:John Wiley & Sons, 2002.

[21] RFDesign RF And Microwave Technology For Design Engineers, "The Principles Of OFDM", Jan 2001, http://rfdesign.com/mag/radioprinciplesofdm/.

[22] A. Gusmão, R. Dinis, J. Conceião, N. Esteves "Comparison of Two Modulation Choices for Broadband Wireless communications" *IEEE 51st Vehicular Technology Conference Proceedings 2000*, pp. 1300-1305, May 2000.

[23] Zhengdao Wang, Xiaoli Ma, Georgios B. Giannakis, "Optimality of Single-Carrier Zero-Padded Block Transmissions", *Wireless Communications and Networking Conference 2002*, pp. 584-588, March 2002.

[24] Thierry Pollet, Mark Van Bladel, Marc Moeneclaey, "BER Sensitivity of OFDM Systems to Carrier Frequency Offset and Wiener Phase Noise", *IEEE Trans. Communications*, vol. 43, pp. 191-193, February/March/April 1995.

[25] Yuping Zhao, Sven-Gustav Häggman, "Intercarrier Interference Self-Cancellation Scheme for OFDM Mobile Communication Systems", *IEEE Trans. Communications*, vol. 49, pp. 1185-1191, July 2001.